GeoExpert ag

swiss*nuclear*: PEGASOS Refinement Project:
SP2 – Ground Motion Characterization

Contract no. PMT-VT-1032

Seismic Shear Wave Velocity Determination and Hybrid Seismic Survey at the SED-Station PLONS (Mels SG)

Date of Field Data Acquisition 14th May 2009

Report

Client

swiss*nuclear*
Project PRP
Frohburgstrasse 17
4601 Olten

Contractor

GeoExpert ag
Seismic Prospecting
Ifangstrasse 12b
P.O. Box 451
8603 Schwerzenbach

8603 Schwerzenbach, 7th July 2009

INDEX

1 INTRODUCTION

1.1 Survey objectives

The seismic survey's main task is to provide information about the distribution function of the shear wave velocities in the depth interval of the uppermost 30 m along a 100 m long seismic profile.

Additionally, the following objectives are to be met:

- the mapping of the topography of the rock face, i.e. the thickness of the Quaternary deposits;
- the determination of the thickness of the weathered zone and its degree of decompaction at the bedrock surface;
- a general view of geological structures.

1.2 The choice of the appropriate surveying methods

Several methods are available for deriving the s-wave velocity distribution in the subsurface at any given position:

- in-situ measurement by down-hole or crosshole seismic surveying;
- shear-wave refraction tomography profiling;
- dispersion analysis of surface waves (MASW; **M**ultiple channel **A**nalysis of **S**urface **W**aves)

The surveys are to be carried out at, or as close as possible near some 20 SED earth quake monitoring stations in Switzerland. Ideally, the surveys are to be conducted on two orthogonal profiles in order to derive at their point of intersection a robust 1D s-wave velocity distribution function by correlation. To this end, the methods of MASW and shear-wave refraction tomography profiling are to be combined.

The results are to include the following fundamental parameters $v_{s,5}$, $v_{s,10}$, $v_{s,20}$, $v_{s,30}$, $v_{s,40}$, $v_{s,50}$, $v_{s,100}$ are to be calculated, also an error estimation of all values.

The data acquired for the MASW method are to be subjected to complementary **p-wave hybrid seismic data processing** in order to image the geological structures.

2 FIELD DATA ACQUISITION PARTICULARS

2.1 Time Schedule

Date	*Time*	*Activities / remarks*
06.05.2009	0845	arrival at site
	0845 - 0915	site investigation
	0915 - 1020	lay-out of spread profile 1 (p-wave and s-wave)
	1020 - 1100	data acquisition of spread profile 1 (p-wave)
	1110 - 1215	data acquisition of spread profile 1 (s-wave)
	1215 - 1300	lay-out of spread profile 2 (p-wave and s-wave)
	1345 - 1410	data acquisition of spread profile 2 (p-wave)
	1430 - 1500	data acquisition of spread profile 2 (s-wave)
	1500 - 1530	removal of the seismic measuring system
	1530	leaving from site

2.2 Summary of Data Acquisition Parameters

Compressional Wave Data Acquisition

# of active channels	96
geophone type	4.5 Hz natural frequency, vertical velocimeter
receiver station spacing	1.0 m
# of geophones/station	1
source point spacing	2.0 m to 3.0 m
source type	vertical hammer (8 kg) striking on a horizontal metal plate
sampling rate	500 µs
recording time	2048 ms
field filters	0.5 Hz LC, anti-alias
# of field records	53 (line 09SN_12PLONS-P1) and 45 (line 09SN_12PLONS-P2)

Shear Wave Data Acquisition

# of active channels	48
geophone type	10 Hz natural frequency, horizontal velocimeter
receiver station spacing	2.0 m
# of geophones/station	1
source point spacing	4.0 m to 6.0 m
source type	horizontal hammer (8 kg) striking horizontally at a metal-plated wooden beam anchored to the ground by means of 20 cm long spikes
sampling rate	500 µs
recording time	512 ms
field filters	2 Hz LC, anti-alias
# of field records	51 (line 09SN_12PLONS-S1) and 48 (line 09SN_12PLONS-S2)

Fig. 2.1: Data acquisition at profile 09SN_12PLONS-1.

2.3 Composition of Seismic Field Crew

Personnel

Jochen Fiseli	Dipl.-Geologist, University of Freiburg i. Br., party chief
Kieron Lynch	assistant, spread lay-out and activation of seismic source
Fabian Isler	assistant, spread lay-out and activation of seismic source

Equipment

96	vertical geophones 4.5 Hz
48	horizontal geophones 12 Hz
6	seismic cables
1	seismic acquisition system Summit Compact, 96 channels
1	laptop computer for data acquisition
3	walkie-talkies
1	hammer 8 kg
1	steel plate
1	metal-plated wooden beam
1	van (FIAT Ducato 4x4)

2.4 Location

The seismic monitoring station PLONS (Mels SG) is situated in Permian sediments (Verrucano), in Eastern Switzerland, canton of St. Gallen.

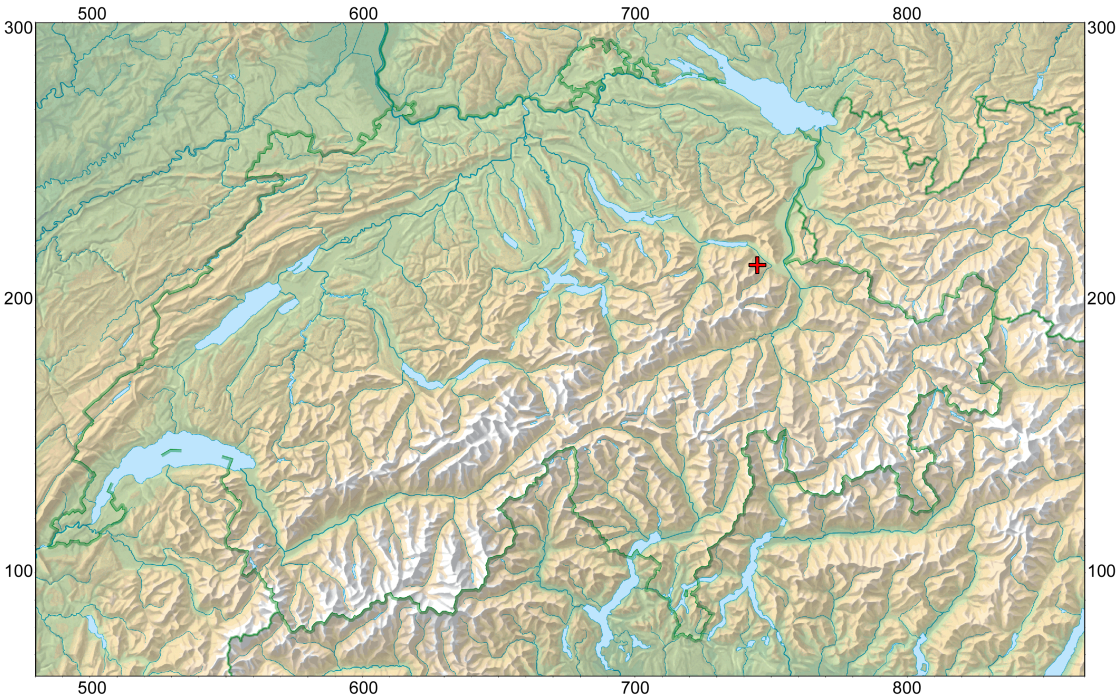

Fig. 2.2: The red cross marked seismic monitoring station PLONS (Mels SG) is located in Permian sediments (Verrucano). (map: geodata @ swisstopo).

2.5 Recording Conditions and Line Setup

Warm temperatures prevailed throughout the field data recording period.

Timber works were responsible for a lot of noise during the data acquisition period. In general, the data quality obtained at PLONS is to be rated as fair.

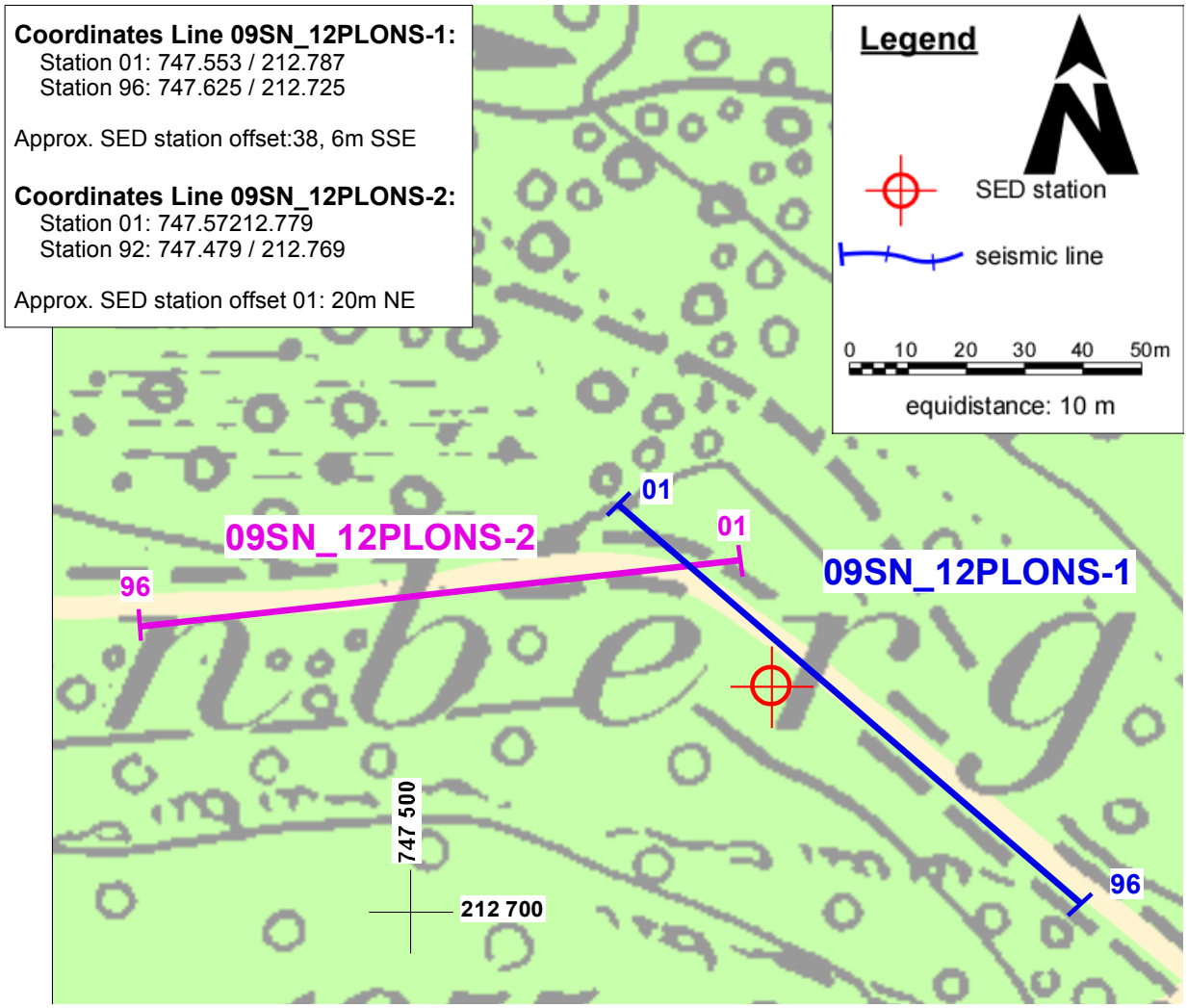

Fig. 2.3: Situation map with the trace of seismic profile 09SN_12PLONS-1 and -2. (background map: ©IG GIS, 08. Jan. 2009; www.geoportal.ch)

3 SEISMIC DATA PROCESSING AND IMAGING OF THE RESULTS

3.1 General Remarks

- For the shear and compressional wave refraction seismic evaluation the package **RAYFRACT** by Intelligent Resources Ltd., Vancouver CAN, was used. The system features the technique of diving wave tomography (www.rayfract.com).
- The system **SPW** (**S**eismic **P**rocessing **W**orkshop) of Parallel Geoscience Corporation, Austin US-TX, was used for reflection seismic data processing (www.parallelgeo.com).
- Data processing of surface waves (MASW processing) was conducted with the software package **SurfSeis** V2.0 of Kansas Geological Survey in Lawrence US-KS.

A detailed description of the various surveying methods will be included in the general summary report.

3.2 Shear Wave Refraction Tomography

3.2.1 Reformatting and field geometry assignment

After reformatting the field data into the Rayfract format the field geometry is applied.

3.2.2 First break time picking

At each shot position, two seismic records were acquired in both activation directions. These two records are displayed superimposed with different colors on each other in Fig 3.2a together with the manually determined first arrival time picks.

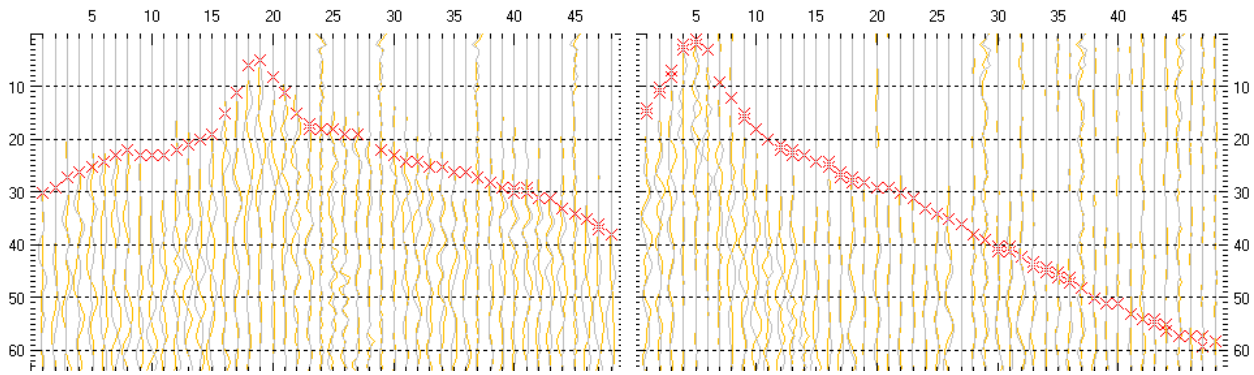

*Fig. 3.2a: High quality dual field record of line 09SN_12PLONS-S1 (left) and -S2 (right) showing at each station the s-wave traces with opposing polarities in different colors. The manually picked s-wave refraction arrivals at each station are marked with an **x**. The station spacing is 2 m, profile station number 00 = profile meter 0; profile station number 48 = profile meter 96.*

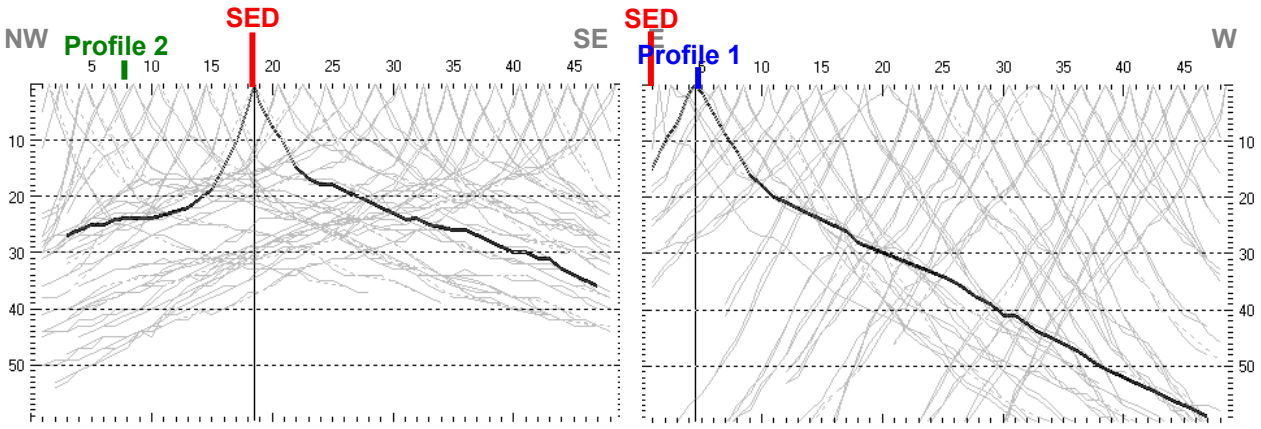

Fig. 3.2b: Curves of s-wave first break time picks of line 09SN_12PLONS-S1 (left) and -S2 (right).

3.2.3 Analytical Determination of Refraction Velocities

An initial 1D-velocity function (averaged 1D velocity-depth profiles derived by the Delta-t-V method, see Tab. 3.2a) is determined in the 3-dimensional time-offset-CMP-domain of all first break arrival time curves in the 3-dimensional time-offset-CMP-domain (see. Fig. 3.2c).

Depth [m]	Vs [m/s]
0.0	395
0.4	451
0.7	478
1.2	575
1.8	718
2.7	1001
3.7	1376
5.3	1940
7.3	2422
10.1	2910
13.7	3203
18.8	3487
25.6	4243
34.6	4639
46.9	4667

Depth [m]	Vs [m/s]
0.0	456
0.5	576
0.9	626
1.4	656
2.1	683
3.4	778
4.8	921
6.9	1141
9.9	1418
14.2	1580
20.1	2570
28.2	3719
39.8	4052

Tab. 3.2a: Initial 1D s-wave velocity function derived from real data of line 09SN_12PLONS-S1 (mean values over all) and of line -S2 (mean values between profile meters 0 and 40).

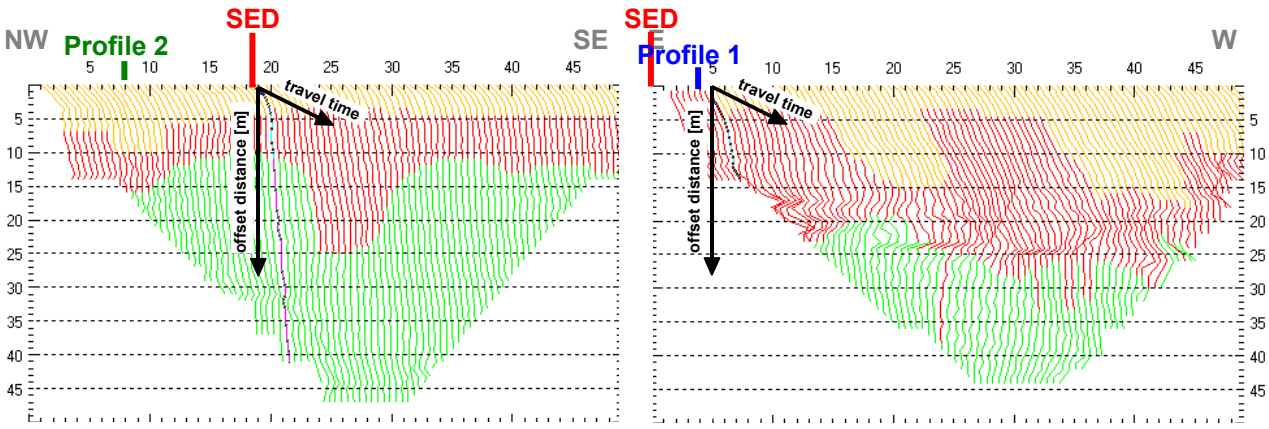

Fig. 3.2c: 3-dimensional distance-travel time diagrams of line 09SN_12PLONS-S1 (left) and -S2 (right) at the mid-points between source points and receiver stations are instrumental when using the analytical CMP derivation of the initial velocity field.
The horizontal axes are the along the CMP positions and the travel time respectively, the vertical axis denotes the offset distance between source and receiver positions. The colors represent different velocity layers. The station spacing is 2 m, profile station number 00 = profile meter 0; profile station number 48 = profile meter 96. The colors represent different velocity layers.

3.2.4 Tomographic inversion of the velocity gradient field by iterative modeling

The velocity field is iteratively refined by the subsequent Wavepath Eikonal Traveltime (WET) tomographic inversion process. The inversion results are portrayed in Fig. 3.2d as a gridded velocity contour section and in Fig. 3.2e as a ray path density section.

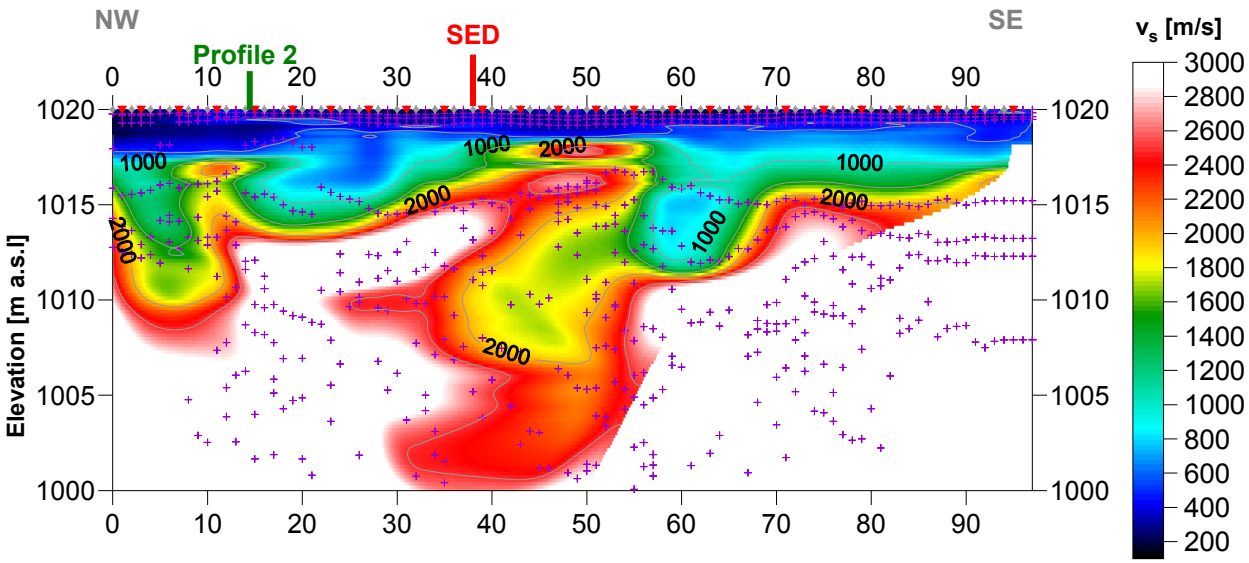

Fig. 3.2d: Shear wave velocity field of the line 09SN_12PLONS-S1. Red/white colors denote solid rock, blue/black colors point to unconsolidated sediments and soil.
Vertical axis: elevation [m a.s.l]; horizontal axis: profile meter; color encoded scale: v_s [m/s]; vertical exaggeration: 2:1; gray diamonds: receiver positions; red triangles: source positions; magenta crosses: positions of determined velocity values. The station spacing is 2 m, profile meter 0 = profile station number 00, profile meter 96 = profile station number 48.

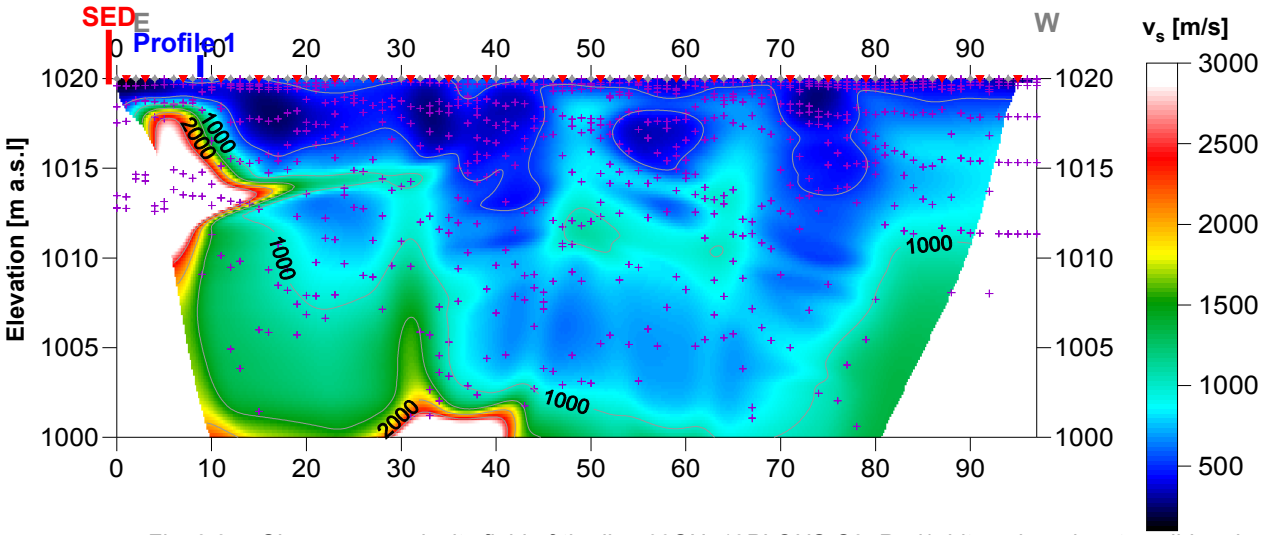

Fig. 3.2e: Shear wave velocity field of the line 09SN_12PLONS-S2. Red/white colors denote solid rock, blue/black colors point to unconsolidated sediments and soil. Vertical axis: elevation [m a.s.l]; horizontal axis: profile meter; color encoded scale: v_s [m/s]; vertical exaggeration: 2:1; gray diamonds: receiver positions; red triangles: source positions; magenta crosses: positions of determined velocity values. The station spacing is 2 m, profile meter 0 = profile station number 00, profile meter 96 = profile station number 48.

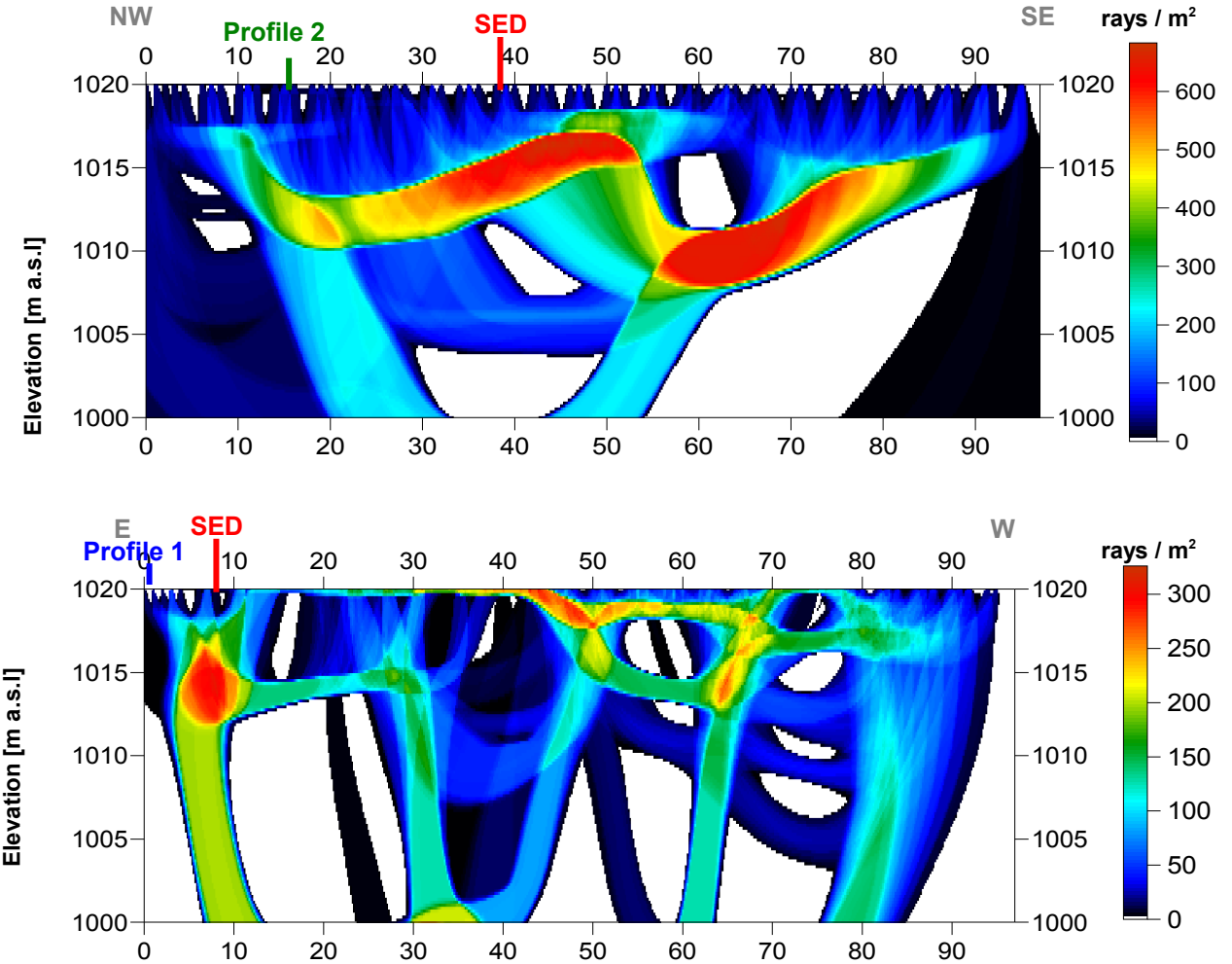

Fig. 3.2f: Shear wave ray path density along the seismic line 09SN_12PLONS-S1 (top) and -S2 (bottom). Red/white colors indicate high velocity contrasts (usually at the bedrock surface), blue/black colors denote low coverage areas. Vertical axis: elevation [m a.s.l]; horizontal axis: profile meter; color encoded scale: ray paths per m²; vertical exaggeration: 2:1. The station spacing is 2 m, profile meter 0 = profile station 00, profile meter 96 = profile station 48.

Depth [m]	Vs [m/s]
0.0	443
1.8	587
3.6	706
5.3	1060
7.1	1061
8.9	951
10.7	929
12.4	947
14.2	975
16.0	1020
17.8	1153
19.5	1733
21.3	2677
23.1	3418
24.9	3169
26.6	3070
28.4	3762

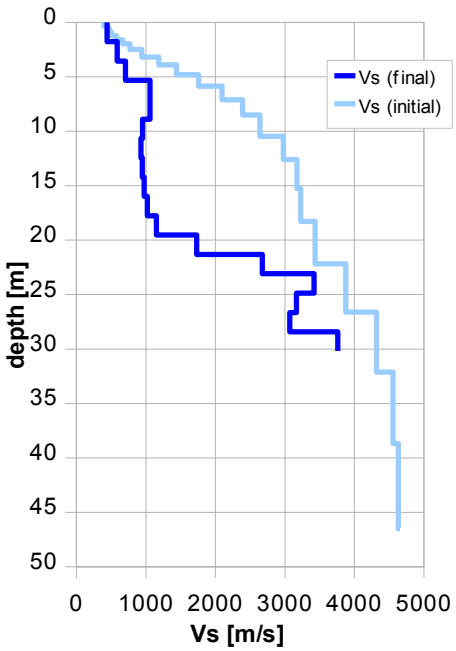

Tab. 3.2b: Final 1D s-wave velocity model derived from real data of line 09SN_12PLONS-S1 (horizontal average of all values) valid for the SED station localization. The calculated values of the initial 1D s-wave velocity model are given in Tab. 3.2a.

Depth [m]	Vs [m/s]
0.0	475
1.8	640
3.6	854
5.3	1615
7.1	1530
8.9	1113
10.7	1063
12.4	1133
14.0	1187
15.8	1244
17.6	1401
19.4	2422
21.1	4281
22.9	5645
24.7	5611
26.5	5568

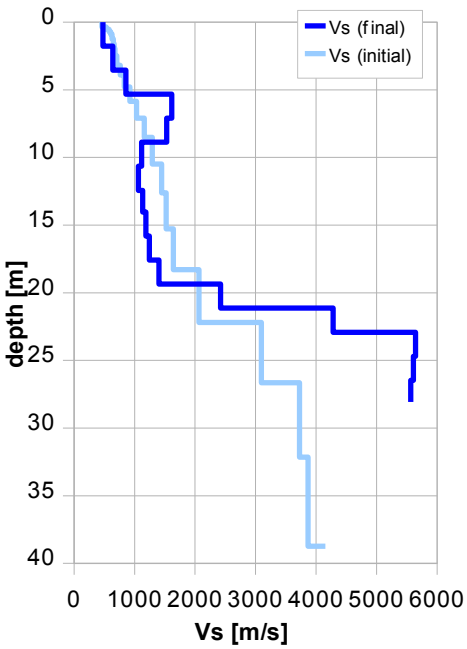

Tab. 3.2c: Final 1D s-wave velocity model derived from real data of line 09SN_12PLONS-S2 (horizontal average of all values) for the profile segment (between profile meters 0 and 40) with a geological setting resembling the one at the SED station. The calculated values of the initial 1D s-wave velocity model are given in Tab. 3.2a.

The highest velocities of more than 4000 m/s seems to be artificial and are not reliable.

3.3 MASW Processing

3.3.1 Reformatting and field geometry assignment

The data preparation steps for the dispersion analysis include

- the assignment of the field acquisition geometry
- the selection of suitable offset ranges (=arrays) between 10 m and 50 m for dispersion, and the splitting of the field records in forward and reverse shooting direction data sets
- the reformatting of the data into the specific KGS format

X - - ... - - o-o-o-...-o-o-o (forward shooting or so-called PLUS direction)
respectively
o-o-o-...-o-o-o - - ... - - X (reverse shooting or so-called MINUS direction).

where **X** = shot position
o = receiver station
- = 1.0 m offset

The active array used at SED-station PLONS are the receiver station in the shot offset range between 10 and 50 m.

3.3.2 Calculating the dispersion image (overtone)

The result of dispersion analysis is the color encoded acoustic energy distribution in the phase velocity - frequency plane (see Fig. 3.3a and b).

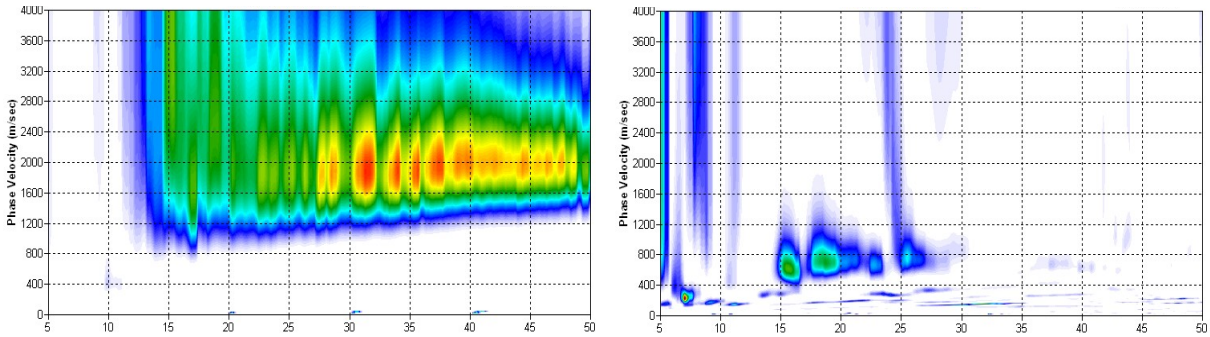

Fig. 3.3a: Dispersion image of perfect quality data (left) from line 09SN_12PLONS-M1 as found on 80 % of that line and of deficient quality data (right) from line 09SN_12PLONS-M2 representing about 80 % of that line of site PLONS.
Horizontal axis: frequency from 5 to 50 Hz; vertical axis: phase velocity from 0 to 4000 m/s; color code: colors from white (no energy) to blue - green - yellow - red - black point to increasing energy amplitude values.

3.3.3 Analysis of the dispersion image

In the dispersion graphs as calculated in section 3.3.2 above, the curves joining the amplitude peaks of the fundamental modes are determined either by subjective inspection or in a semi-automated manner. On datasets with poorly defined amplitude peaks or with a highly irregular alignment of the peaks, the danger of obtaining improbable or wrong results is real and can only be mitigated by the processing experience and the a-priori knowledge of the geological setting by the geophysicist responsible for the data evaluation.

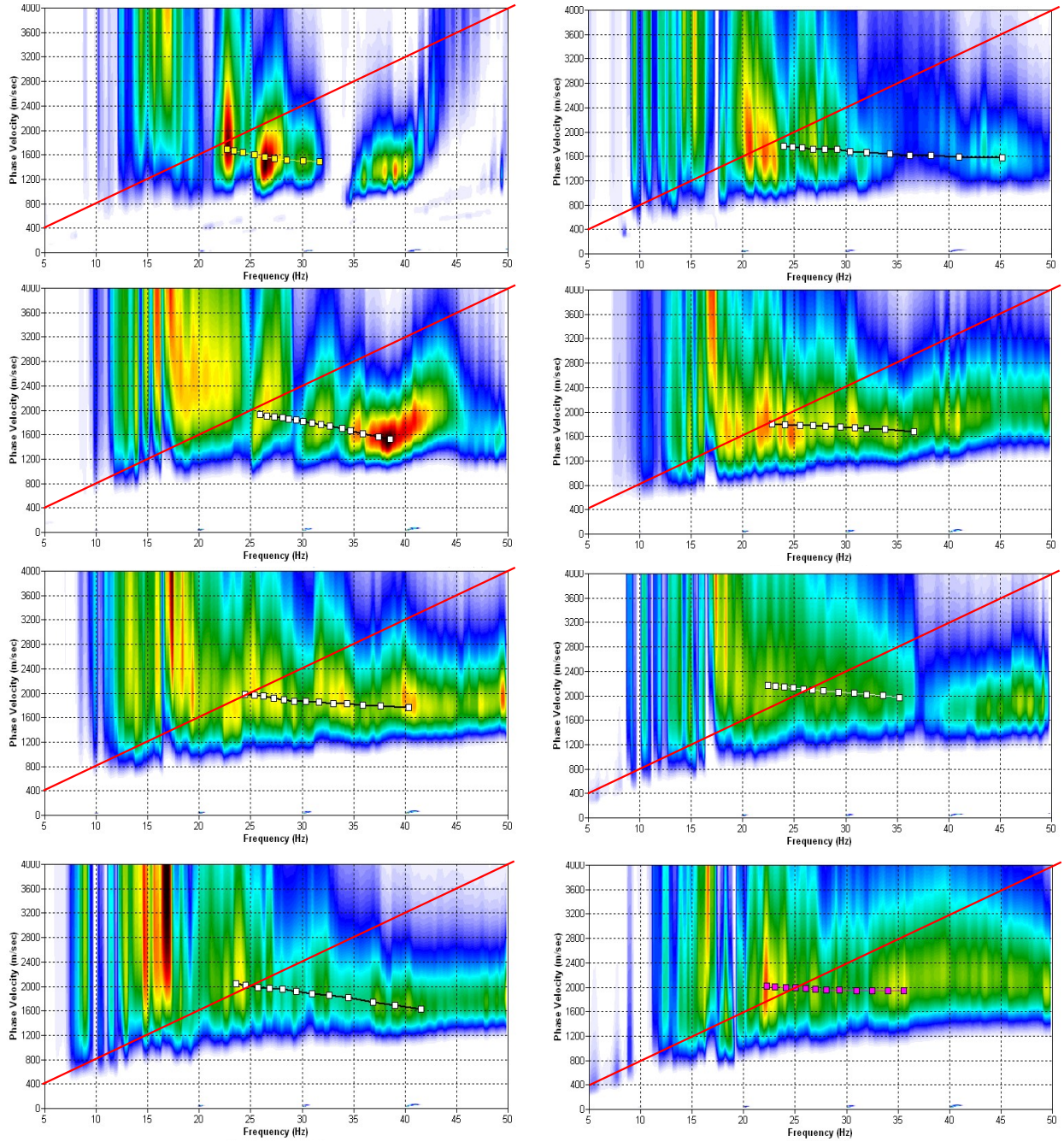

Fig. 3.3b: The manually picked dispersion images used for the derivation of the shear wave velocity section on line 09SN_12PLONS-M1. The dispersion curves (squares) are determined by linking the peaks of high energy. Note that 'higher modes' may at times produce higher energy peaks than the fundamental mode required for the analysis.
dotted fine line: signal-noise ratio for the designated f-v_{ph} – value.
red line: high resolution beam-forming curve for v_{max}.
1st row: left: station 31 @ PLUS direction; right: station 20 @ MINUS direction
2nd row: left: station 45 @ PLUS direction; right: station 35 @ MINUS direction
3rd row: left: station 60 @ PLUS direction; right: station 57 @ MINUS direction
4th row: left: station 75 @ PLUS direction; right: station 73 @ MINUS direction

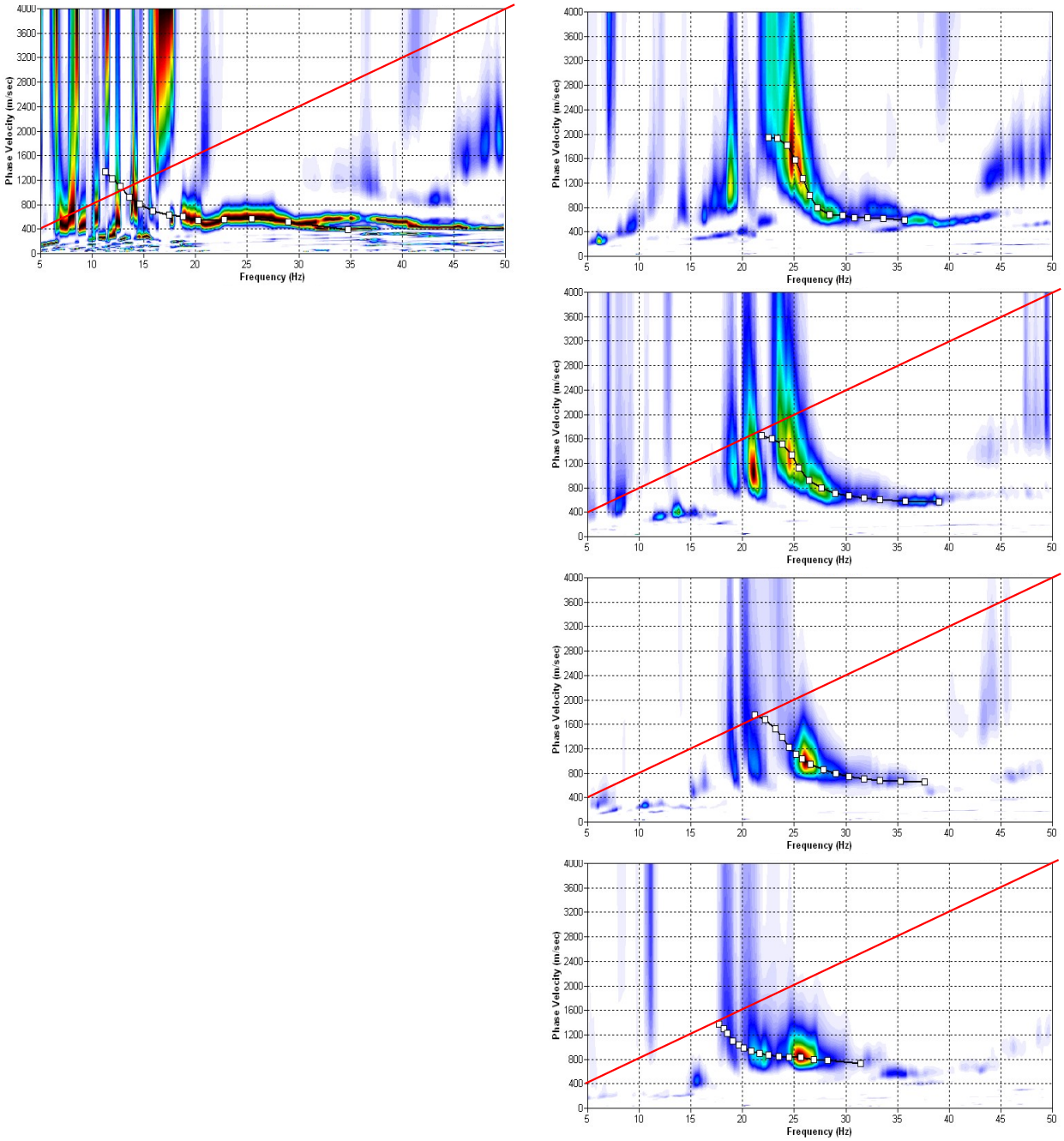

Fig. 3.3c: The manually picked dispersion images used for the derivation of the shear wave velocity section on line 09SN_12PLONS-M2. The dispersion curves (squares) are determined by linking the peaks of high energy. Note that 'higher modes' may at times produce higher energy peaks than the fundamental mode required for the analysis.
dotted fine line: signal-noise ratio for the designated f-v_{ph} – value.
red line: high resolution beam-forming curve for v_{max}.
1st row: left: station 40 @ PLUS direction; right: station 24 @ MINUS direction*
2nd row: left: not available; right: station 30 @ MINUS direction
3rd row: left: not available; right: station 36 @ MINUS direction
4th row: left: not available; right: station 39 @ MINUS direction

** this dispersion plot gives vertical normalized amplitudes*

3.3.4 Inversion of dispersion curves resulting in a 1D shear wave velocity distribution

Inversion of the extracted dispersion curves was performed using the algorithm described by Xia et al. (1999).

The inversion process is started by setting the maximum depth (z_{max}) to be in the order of 30% of the largest wavelength for an initial model consisting of 10 layers of increasing thicknesses. For all 10 layers the Poisson's ratio is assumed to be 0.4 and the rock/soil density to be 2.0 g/cm^3. The inversion process is concluded either after twelve iterations or when the convergence condition of a RMS-error of less than 3 m/s (phase velocity) is met.

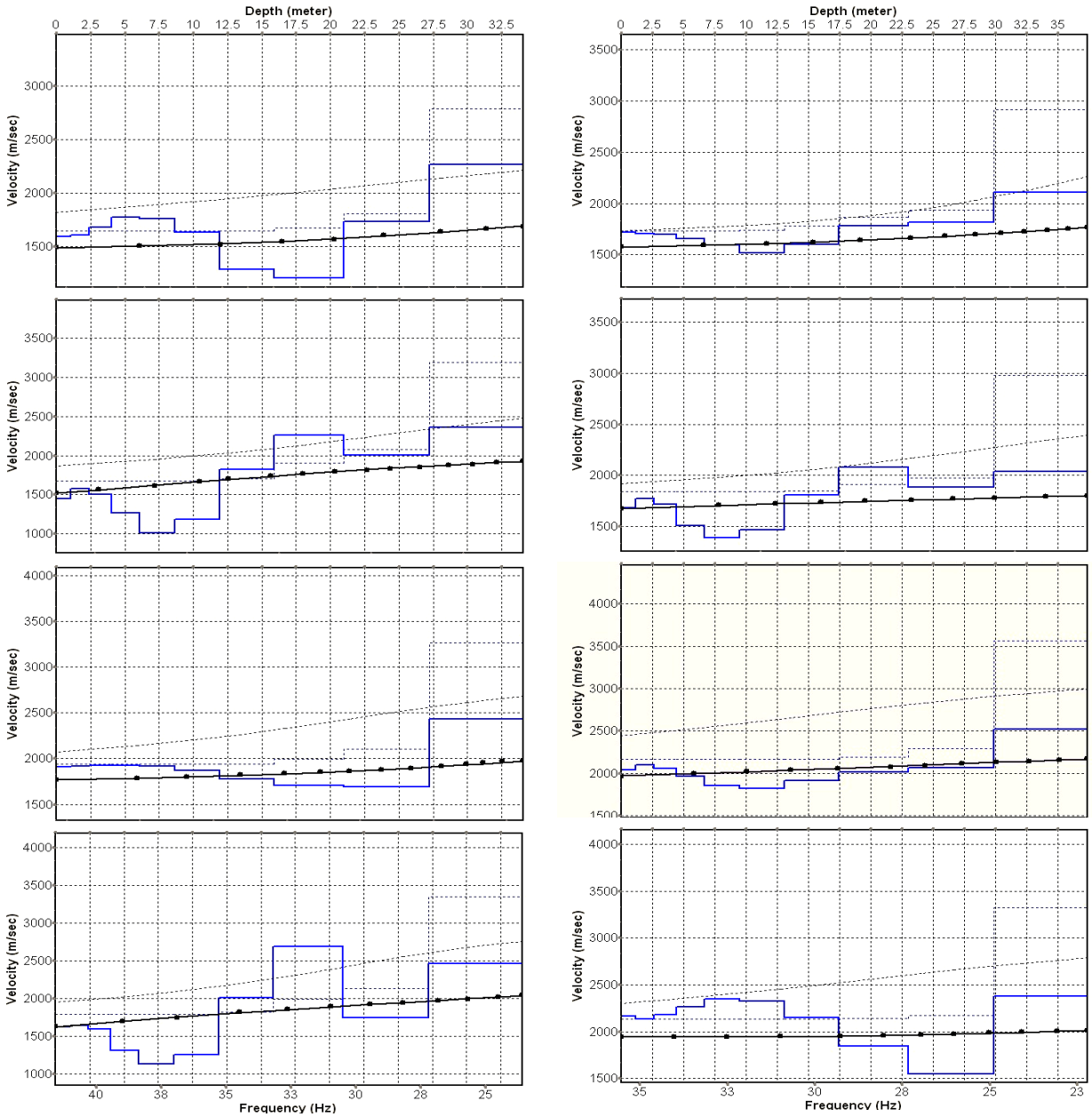

Fig. 3.3d: Inversion results of dispersion curves of dataset at line 09SN_12PLONS-M1.
***brown**: Inversion of dispersion curve (dots) resp. of the modeled dispersion curve (dotted line: initial model; continuous line: end model). Horizontal axis: frequency Hz, vertical axis: v_s.*
***blue**: 10-layer-model (dotted: initial model, continuous line: final model). Horizontal axis: depth, vertical axis: phase velocity resp. v_s).*
1st row: left: station 31 @ PLUS direction; right: station 20 @ MINUS direction
2nd row: left: station 45 @ PLUS direction; right: station 35 @ MINUS direction
3rd row: left: station 60 @ PLUS direction; right: station 57 @ MINUS direction
4th row: left: station 75 @ PLUS direction; right: station 73 @ MINUS direction

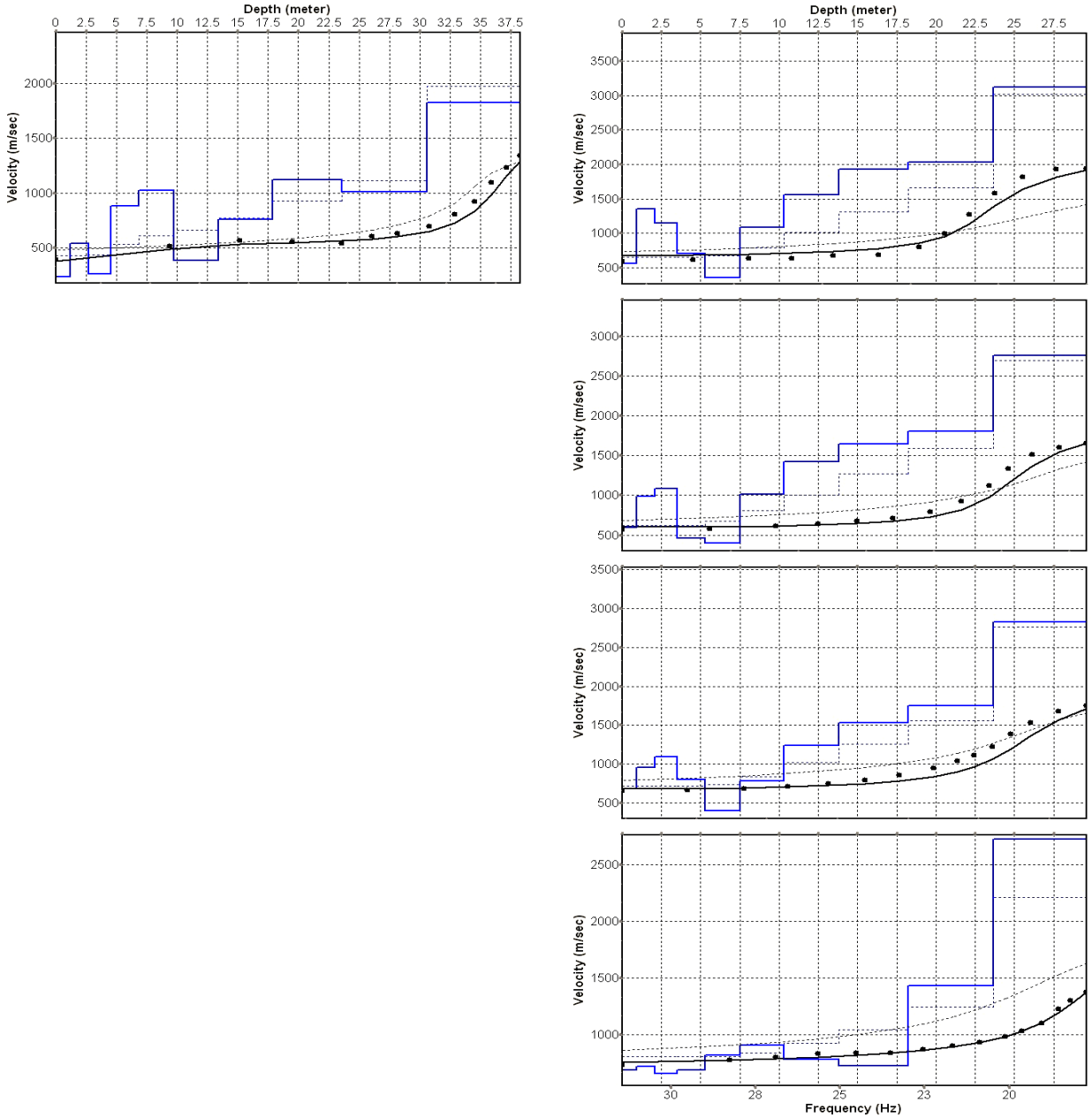

Fig. 3.3e: Inversion results of dispersion curves of dataset at line 09SN_12PLONS-M2.
***brown**: Inversion of dispersion curve (dots) resp. of the modeled dispersion curve (dotted line: initial model; continuous line: end model). Horizontal axis: frequency Hz, vertical axis: v_s.*
***blue**: 10-layer-model (dotted: initial model, continuous line: final model). Horizontal axis: depth, vertical axis: phase velocity resp. v_s).*
1st row: left: station 40 @ PLUS direction; right: station 24 @ MINUS direction
2nd row: left: not available; right: station 30 @ MINUS direction
3rd row: left: not available; right: station 36 @ MINUS direction
4th row: left: not available; right: station 39 @ MINUS direction

Dispersion analyses of records with longer receiver arrays should – by theory – increase the investigation depth. At PLONS, with both lines and both directions, MASW processing with the maximal array length of 96 m verify the results from 40-m-arrays resp. gives a reliable v_S-model on line M2 (only in PLUS direction) (Fig. 3.3f and 3.3g).

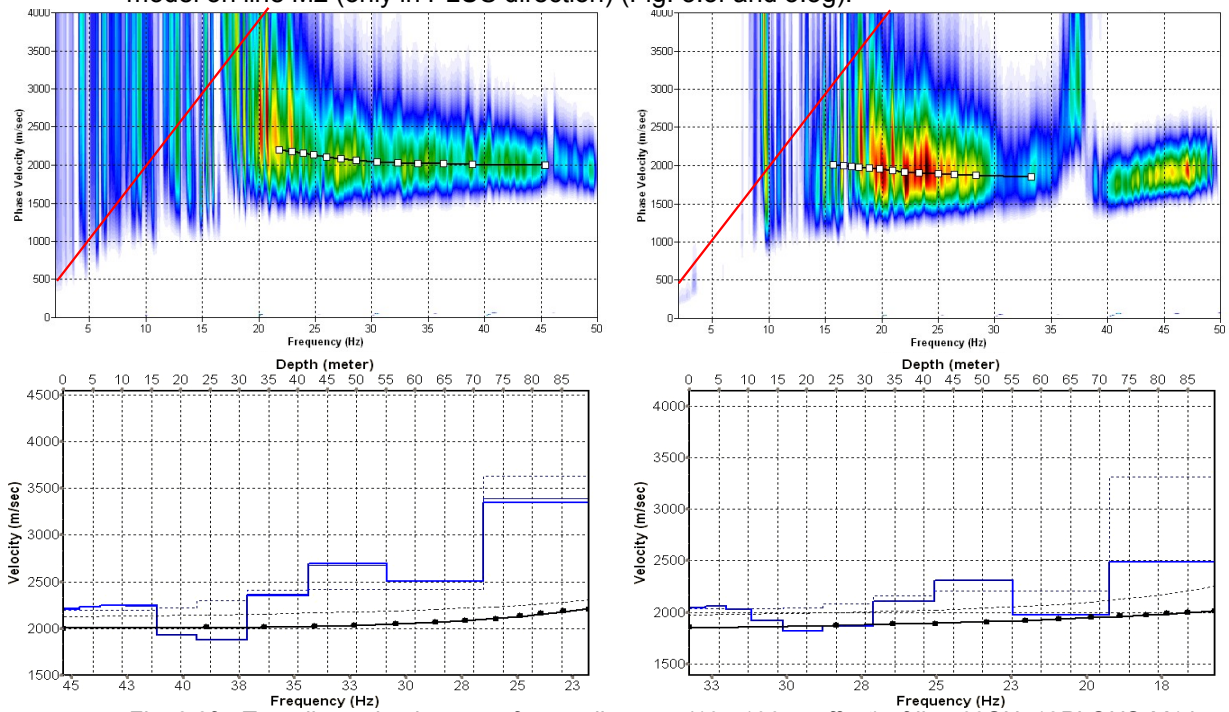

Fig. 3.3f: Top: dispersion images of over-all arrays (10...106 m offset) of line 09SN_12PLONS-M1 in PLUS (left) and MINUS (right) direction; dotted fine line: signal-noise ratio for the designated f-v_{ph}-value. Red line: high resolution beam-forming curve for v_{max}.
*Below: The two respective inversion results; **brown**: inversion of dispersion curve; **blue**: 10-layer-model. Horizontal axis: depth, vertical axis: phase velocity resp. v_S.*

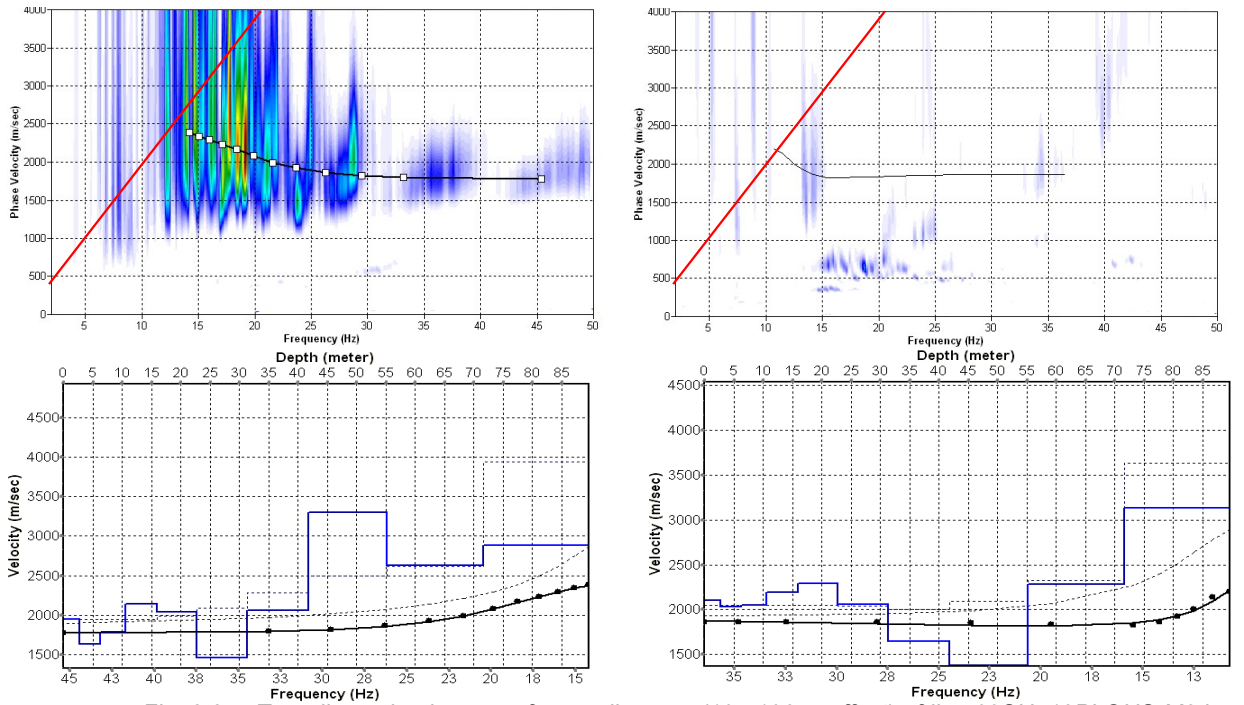

Fig. 3.3g: Top: dispersion images of over-all arrays (10...106 m offset) of line 09SN_12PLONS-M2 in PLUS (left) and MINUS (right) direction; dotted fine line: signal-noise ratio for the designated f-v_{ph} – value. Red line: high resolution beam-forming curve for v_{max}.
*Below: The two respective inversion results; **brown**: inversion of dispersion curve; **blue**: 10-layer-model. Horizontal axis: depth, vertical axis: phase velocity resp. v_S.*

3.3.5 Gridding and plotting of 2D v_s-velocity field

By assembling the 1D v_s - depth functions of all stations the final 2D v_s-field is derived using a Kriging gridding procedure as portrayed in Fig. 3.3h and 3.3i below:

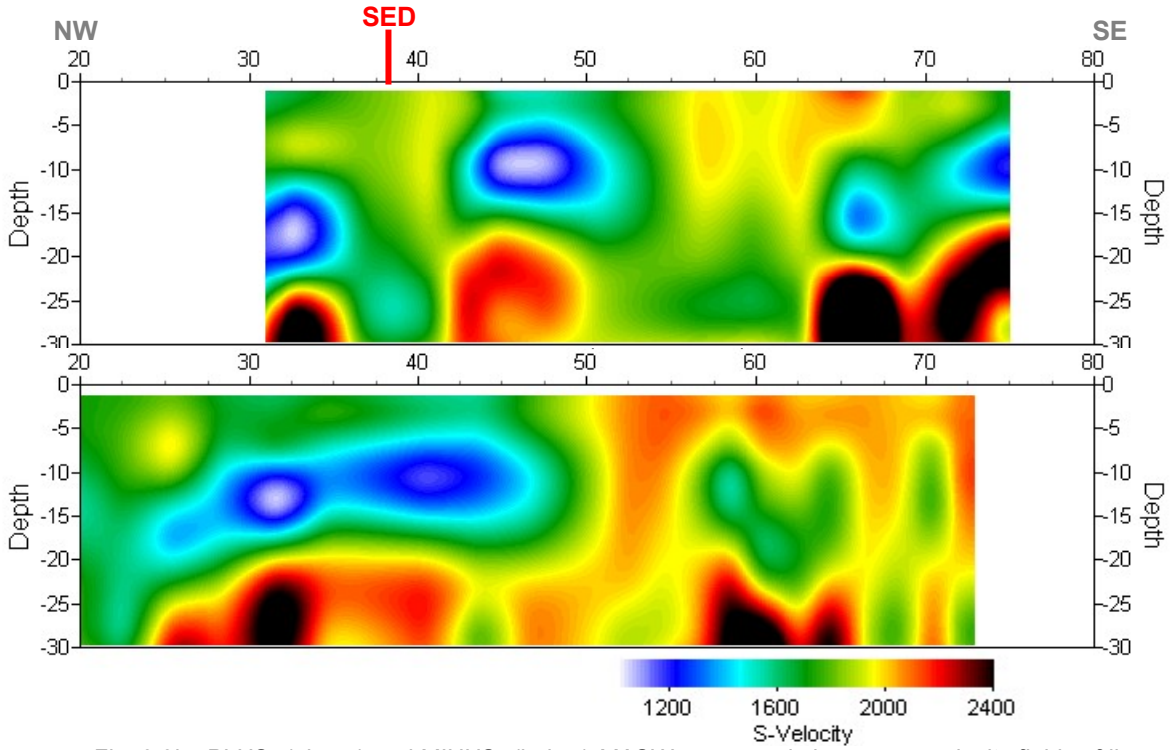

Fig. 3.3h: PLUS- (above) and MINUS- (below)-MASW-processed shear wave velocity fields of line 09SN_12PLONS-M1. Station spacing is 1 m.

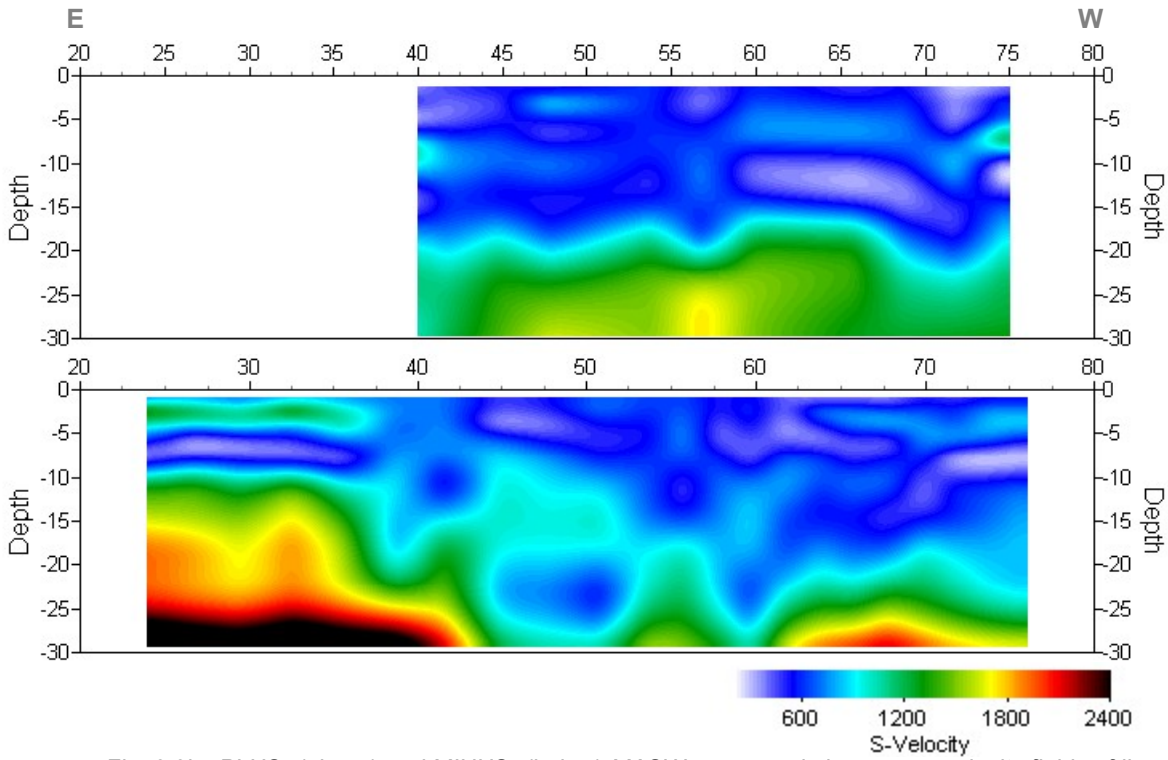

Fig. 3.3i: PLUS- (above) and MINUS- (below)-MASW-processed shear wave velocity fields of line 09SN_12PLONS-M2. Station spacing is 1 m.

3.3.6 Calculation of the average shear wave velocity

In order to calculate a representative shear wave velocity-depth function of line 09SN_12PLONS-M1 at the SED station, all computed 1D-v_S-depth functions are averaged (non-weighted mean values). The v_S-depth-function is shown in Tab. 3.3a.

Depth [m]	Vs- [m/s]	Vs- [m/s]	Vs [m/s]
1.1	1874	1799	1836
2.5	1908	1814	1861
4.2	1900	1801	1851
6.4	1836	1740	1788
9.1	1736	1647	1692
12.5	1671	1600	1636
16.7	1755	1666	1710
22.0	1959	1882	1921
28.6	2078	2062	2070
35.7	2240	2148	2194

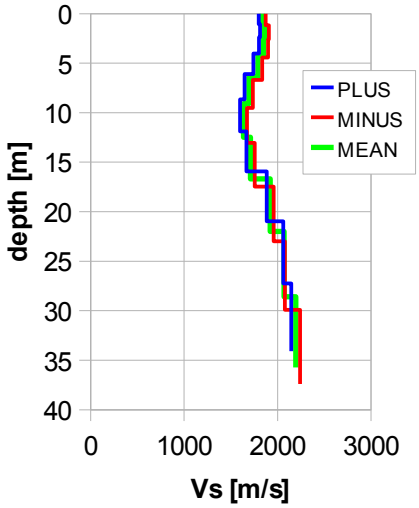

Tab. 3.3a: Averaged vs - depth function of line 09SN_12PLONS-M1 at the SED station. Blue line: MASW-'PLUS' processing, red line: MASW-'MINUS' processing; green line: average of PLUS- and MINUS-functions.

In order to calculate an representative shear wave velocity-depth function of line 09SN_12PLONS-M2 at the SED station, all computed 1D-v_S-depth functions between seismic profile station no. 0 and 40 are averaged (non-weighted mean values). (In PLUS directions, that is only one function.) The resulting v_S-depth-function is shown in Tab. 3.3b.

Depth [m]	Vs- [m/s]	Vs+ [m/s]	Vs [m/s]
1.1	625	240	432
2.4	1097	540	819
4.0	1004	264	634
6.1	583	886	734
8.6	466	1028	747
11.9	1041	386	713
15.9	1374	760	1067
20.9	1594	1123	1358
27.2	1820	1011	1416
34.0	2900	1825	2363

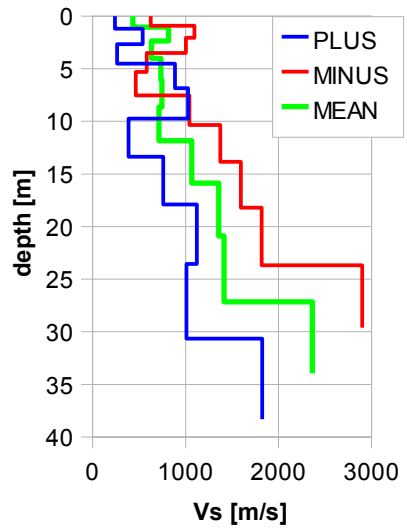

Tab. 3.3b: Averaged v_S - depth function of line 09SN_12PLONS-M2 at the SED station. Blue line: MASW-'PLUS' processing, red line: MASW-'MINUS' processing; green line: average of PLUS- and MINUS-functions.

The inversion of the four 100 m-array dispersion curves data (20 to 116 m offset, see Fig. 3.3f and 3.3g) are given in Tab. 3.3c. These values are complemented with the values derived of the 40 m-arrays analyses (Tab. 3.3a and 3.3b).

100 m array								40 m array			
depth	m1+	m1-	m2+	m2-	m1	m2	m	depth	m1	m2	m
2.8	2209	2045	1952	2107	2127	2029	2069	1.1	1836	432	1134
6.3	2233	2060	1637	2034	2146	1836	1977	2.5	1861	819	1340
10.6	2247	2030	1783	2044	2138	1914	2020	4.2	1851	634	1242
16.0	2246	1921	2139	2195	2083	2167	2102	6.4	1788	734	1261
22.8	1929	1821	2038	2290	1875	2164	1929	9.1	1692	747	1219
31.3	1875	1862	1463	2059	1869	1761	1733	12.5	1636	713	1175
41.9	2359	2106	2065	1648	2233	1856	2177	16.7	1710	1067	1389
55.2	2690	2310	3295	1377	2500	2336	2765	22.0	1921	1358	1639
71.7	2506	1975	2625	2278	2241	2451	2369	28.6	2070	1416	1743
89.7	3351	2490	2885	3132	2920	3008	2909	35.7	2194	2363	2278

Tab. 3.3c: v_s-depth values of the four MASW-derived dispersion curves of both seismic line 09SN_12PLONS-M1 and 09SN_12PLONS-M2 using 100 m-arrays. The dispersion curves are shown in Fig. 3.3f and Fig 3.3g.

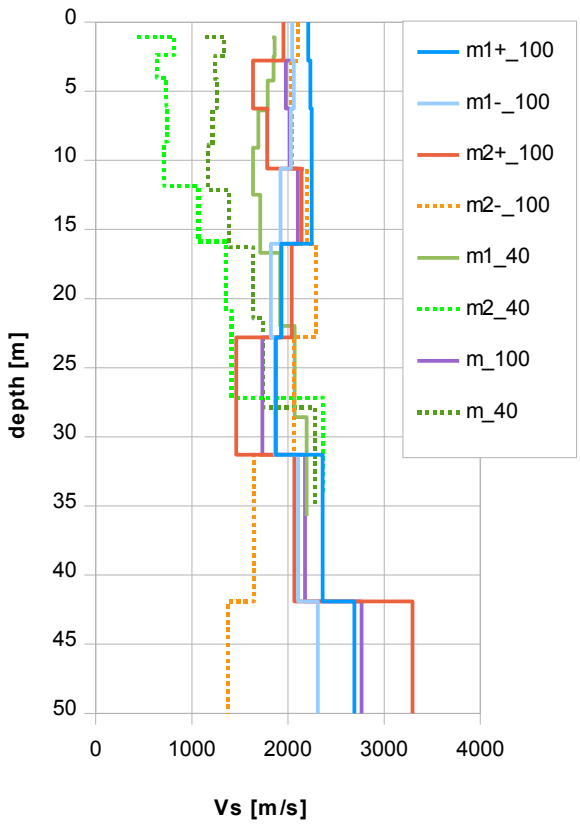

Fig. 3.3j: Comparison of the ensemble of inversion results of both lines 09SN_12PLONS-M1 and -M2, either using the 40 m- and the 100 m-arrays.
blue lines: analyses of records of line 09SN_12PLONS-M1
red lines: analyses of records of line 09SN_12PLONS-M2
magenta line: mean of both 100 m-array records analyses in MINUS and PLUS direction.
green lines: v_s-values of analyses of 40 m-array records.
dotted lines: inversions with low quality values

3.3.7 Calculation of the shear wave velocity scalars $v_{s,5}$, $v_{s,10}$, ...

The parameters $v_{s,5}$, $v_{s,10}$, $v_{s,20}$, $v_{s,30}$, $v_{s,40}$, $v_{s,50}$ represent the average shear wave velocities in the depth interval between the surface and the respective depth levels and are determined from the formula

$$v_{s,n} = \frac{\sum_{i=1}^{n} d_i}{\sum_{i=1}^{n} d_i / v_{si}}$$

with:

d_i = thickness of layer I

v_{si} = corresponding shear-wave velocity.

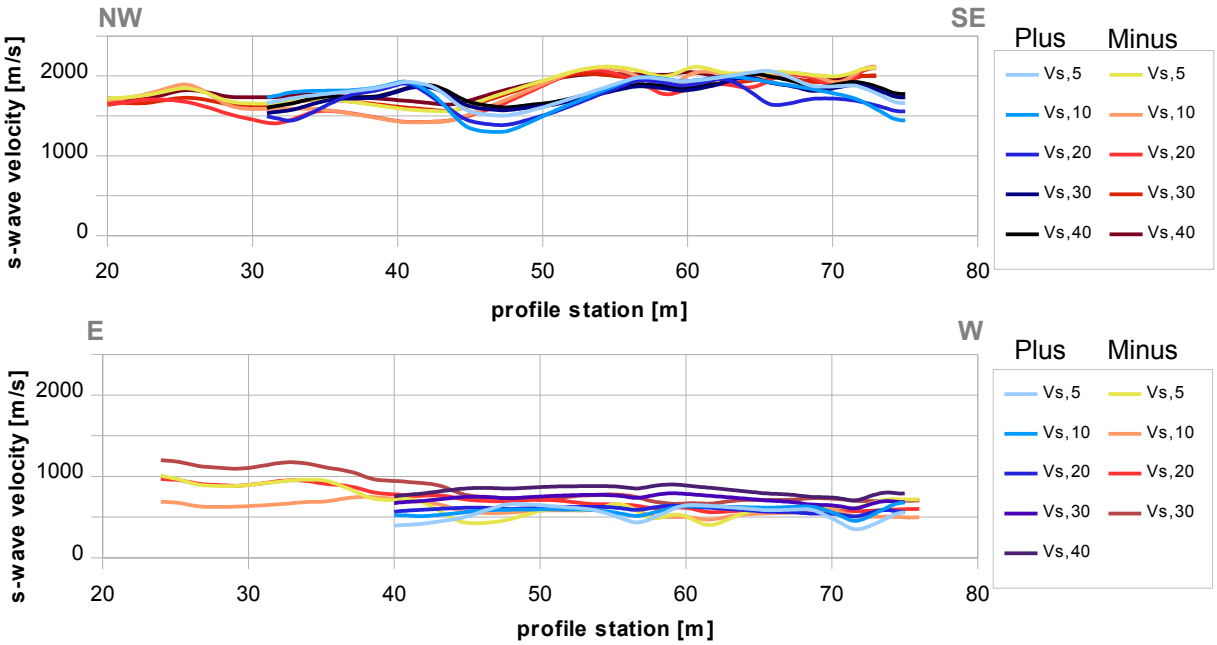

Fig. 3.3l: Graphs of the averaged vs,5...-values along the line 09SN_12PLONS-M1 (top) and -M2 (bottom) for the PLUS- (blue lines) and MINUS- (red lines) directions.

The average values of the s-wave velocity model $v_{s,5}$, $v_{s,10}$, $v_{s,20}$, $v_{s,30}$, $v_{s,40}$, $v_{s,50}$, $v_{s,100}$ (= average shear wave velocity from the surface to depths of 5 m, …until 100 m) on the line segment nearest to the SED station (Tab. 3.3d) are summarized below:

	Vs,5	Vs,10	Vs,20	Vs,30	Vs,40	Vs,50
MINUS	1854	1792	1725	1797	1856	n/a
PLUS	1817	1753	1692	1767	1805	n/a
MEAN	1836	1772	1709	1782	1830	n/a

	Vs,5	Vs,10	Vs,20	Vs,30	Vs,40	Vs,50
MINUS	880	680	893	1095	n/a	n/a
PLUS	402	521	575	681	767	n/a
MEAN	641	600	734	888	767	n/a

Tab. 3.3d: The average shear wave velocities within the depth intervals from surface down to 5 m, etc.… to 50 m, calculated for the line segment with a subjectively most similar geology to the SED station (over all profile station on line 09SN_12PLONS-M1, top; profile stations 0 to 40 for line 09SN_12PLONS-M2, bottom).

3.4 Hybrid Seismic Data Processing

3.4.1 p-wave *Reflection* Seismic Processing Sequence

A) Data conditioning

A1 Reformatting and quality verification of field data
A2 Recording geometry assignment
A3 Data editing (suppression of bad / dead traces, etc.)
A4 Preliminary analysis of refraction velocities

B Filtering and deconvolution

B1 Analytical muting of refraction arrivals
B2 Amplitude recovery / amplitude equalization in time and frequency domains
B3 Predictive deconvolution parameter tests / application
B4 Determination of band limiting corner frequencies / application
B5 Optional 2-D filtering

C) Velocity analysis and stack

C1 Common Depth Point (CDP) sort
C2 Semblance velocity analysis using supergathers of 3 - 5 CDP's
C3 Optional dip move-out correction
C4 Normal Move-Out (NMO) correction and application of stretch mute
C5 Band-pass filtering
C6 CDP stack
C7 Optional coherency filtering

D) Time-depth conversion

D1 Optional spiking deconvolution
D2 Band-pass filtering
D3 Depth conversion
D4 Final display of seismic depth section with inversed polarity (non-SEG-convention)

3.4.2 The presentation of reflection seismic data

The data in a reflection seismic section are presented as an assembly of individual seismic signals at regular intervals along a seismic profile. The simplest way of representing the signals are single wiggle lines (first to the left in the illustration below). A more capturing presentation is the variable area form (second to the left). Combining these two modes results in the var-wiggle mode. Another method of data visualization is the variable density mode (second from the right).

The compressional phase of seismic signals is defined in this report as the onset of the positive amplitude excursion in black (Fig. 3.4a). Since the source signal is produced by an explosion or by an impact at the surface, the signal starts off with a compression of the ground particles. Thus the arrivals of reflection events are defined by the compressional phase.

In rare situations of velocity inversions, cases in which formation velocities are lower than in the layers above, polarity reversals of the reflected signals occur. The beginning of the reflection event would then be characterized by a dilatational phase, represented in this report as a negative amplitude excursion, i.e. in white.

The final p-wave seismic depth sections are displayed in Fig. 3.4b and 3.4c, the hybrid sections in Fig. 3.4j and -k further below.

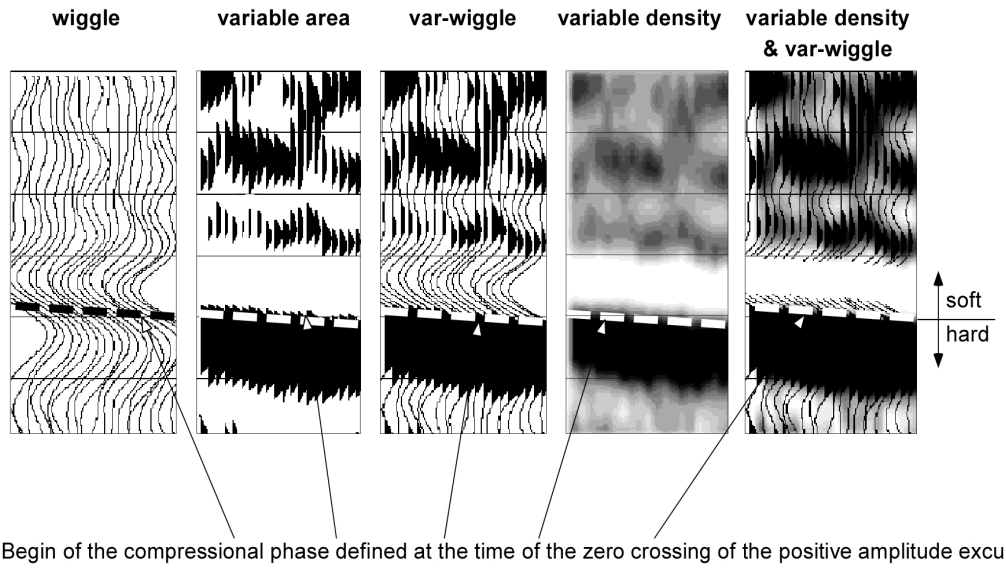

Fig. 3.4a Representation of reflection seismic data and the definition of a reflection event.

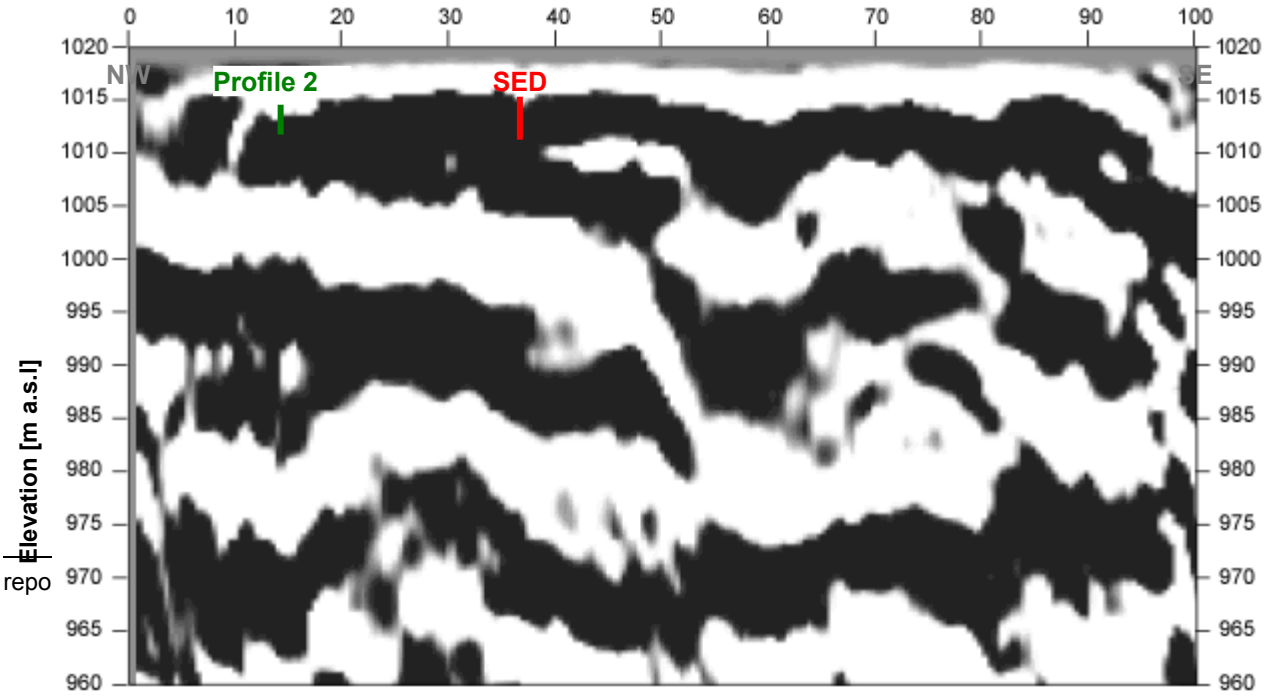

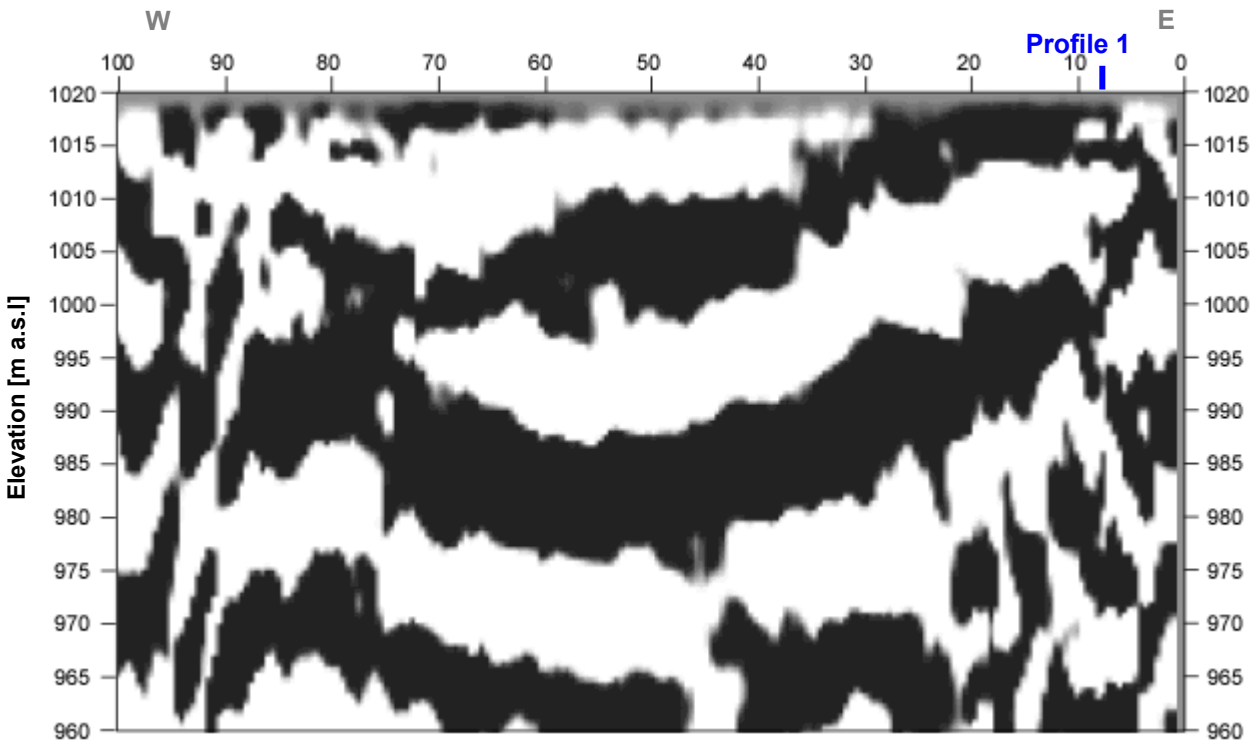

Fig. 3.4c: Seismic depth section of seismic line 09SN_112PLONS-P1 with variable density mode presentation. Vertical axis: elevation [m a.s.l.], horizontal axis: profile meter; no vertical exaggeration. The station spacing is 1 m.

3.4.3 p-wave refraction tomography processing

The seismic p-wave refraction processing steps are analogous to those described in paragraph 3.2. For a detailed method statement and a description of the processing steps please refer to the summary report. The Figs. 3.4d to 3.4i and Tab. 3.4a illustrate the intermediate processing steps and the final result.

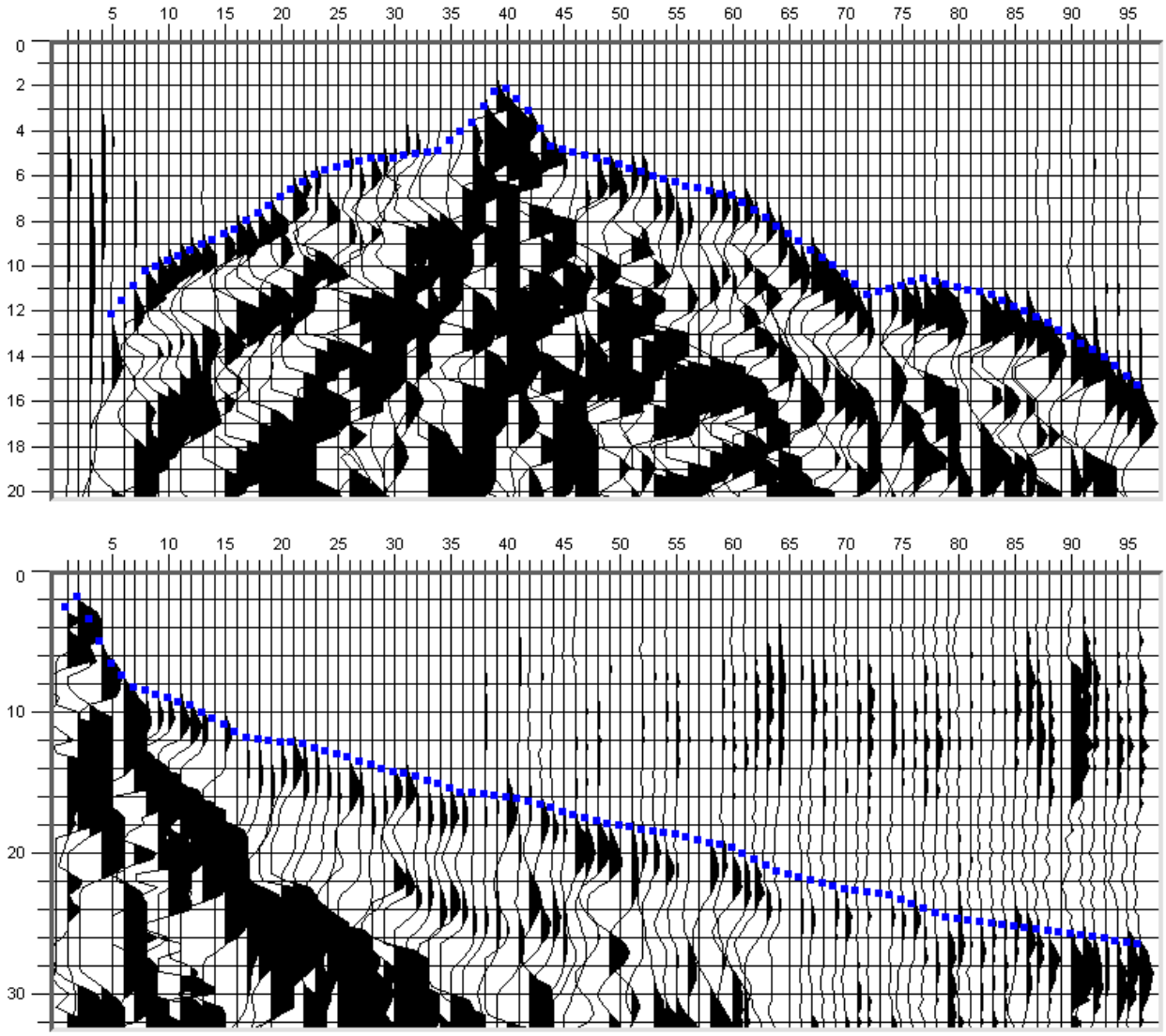

Fig. 3.4d: p-wave records of 09SN_12PLONS-P1 (top) and -P2 (bottom) with positive amplitude excursions in black. Colored dots mark the manually picked first break arrival times. Vertical axis: travel time in ms, horizontal axis: station numbers spaced at 1 m.

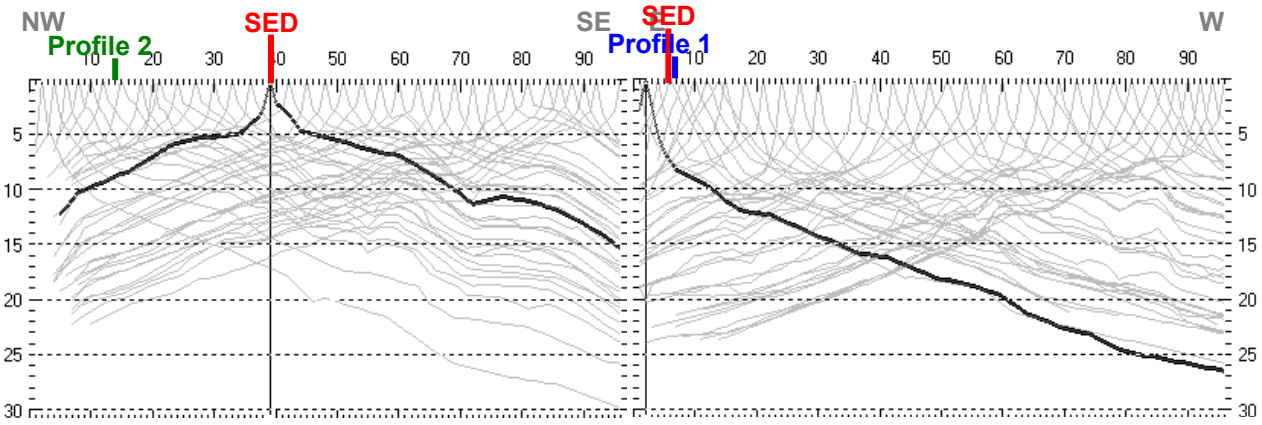

Fig. 3.4e: Travel time curves of p-wave arrival time picks of line 09SN_12PLONS-P1 (left) and -P2 (right). Vertical axes: travel time [ms], horizontal axes: station number (= profile meter).

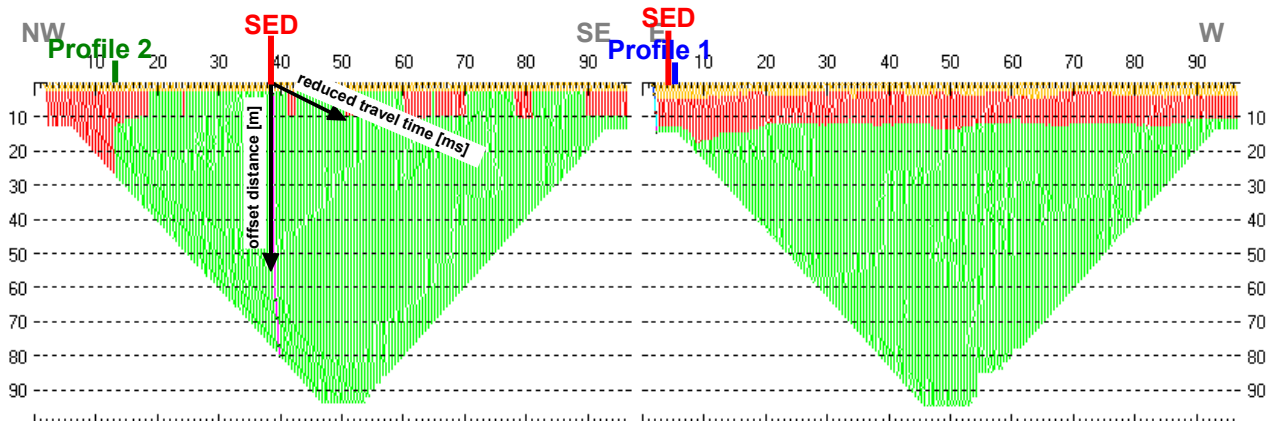

Fig. 3.4f: 3-dimensional distance-travel time diagrams at the mid-points between source points and receiver stations are instrumental when using the analytical CMP derivation of the initial velocity field. The horizontal axes are along the CMP positions and the travel time respectively, the vertical axis denotes the offset distance between source and receiver positions.

Depth [m]	Vp [m/s]
0.0	385
0.1	525
0.3	729
0.7	988
1.0	1351
1.3	1973
1.9	2587
2.8	3724
3.7	4079
4.9	4279
6.5	4441
8.9	4438
11.7	4647
15.5	4184
20.7	4333

Depth [m]	Vp [m/s]
0.0	360
0.1	464
0.3	643
0.5	631
0.7	781
1.0	1027
1.5	1251
2.0	1637
2.7	2282
3.6	2666
4.8	4070
6.4	5076
8.4	4781
11.0	4879
14.4	5414
18.8	5061

Tab. 3.4a: Initial 1D p-wave velocity model derived from real data (left: 09SN_12PLONS-P1; right: -P2).

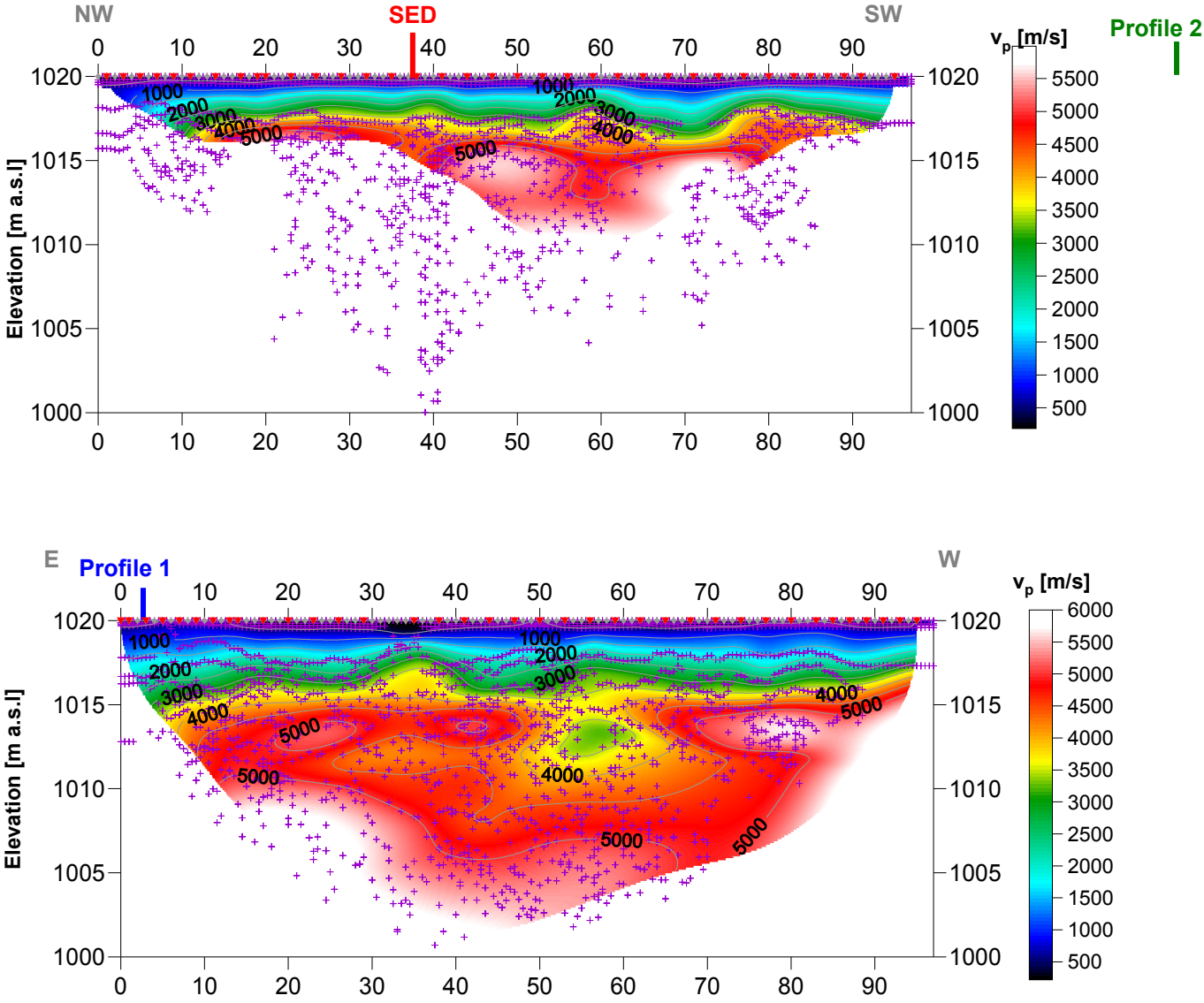

Fig. 3.4g: Compressional wave velocity field image along the seismic profiles 09SN-12PLONS-P1 (top) and -P2 (bottom). Red/white colors indicate solid rock, blue/black colors unconsolidated sediments and soil. Vertical axis: elevation [m a.s.l]; horizontal axis: profile meter; color scale: v_s [m/s]; vertical exaggeration: 2:1; gray squares: receiver stations; red triangles: shot positions; magenta crosses: positions of determined velocity values.

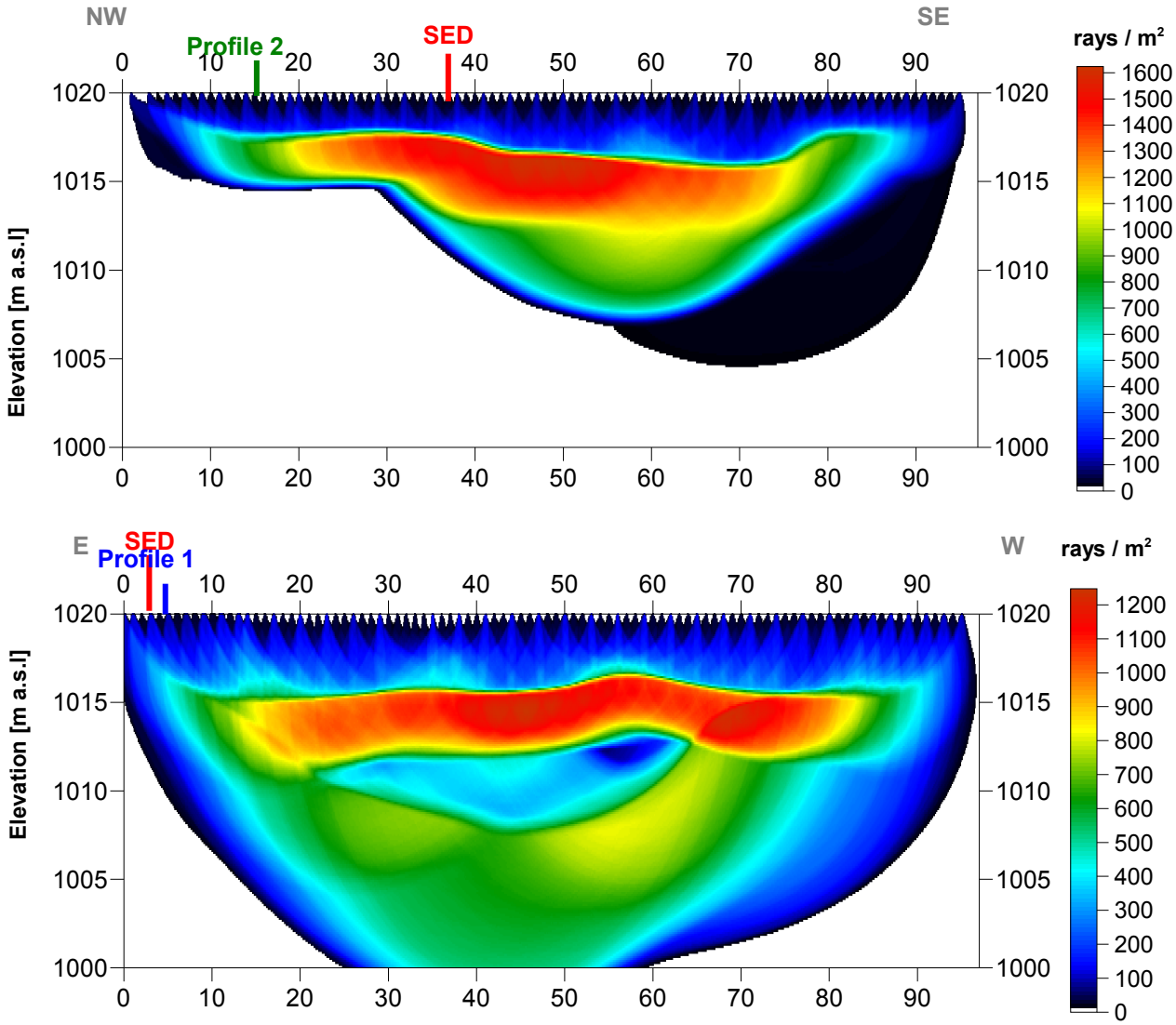

Fig. 3.4h Compressional wave subsurface ray path density along the seismic profiles 09SN_12PLONS-P1 (top) and -P2 (bottom). Red/white colors indicate high velocity contrast between two layers, blue/black colors low coverage areas. Vertical axis: elevation [m a.s.l]; horizontal axis: profile meter; color scale: ray paths per m2; vertical exaggeration: 2:1.

Depth [m]	Vp [m/s]
0.0	417
0.7	999
1.2	1751
1.8	2459
2.3	3079
2.9	3699
3.4	4167
4.0	4343
4.5	4816
5.1	5195
5.7	5373
6.2	5377
6.8	5309
7.3	5269
7.9	5282
8.4	5420
9.0	5599
9.5	5768
10.0	5883

Depth [m]	Vp [m/s]
0.0	339
1.0	953
2.0	1909
3.1	2685
4.1	3325
5.1	4080
6.1	4675
7.1	4744
8.1	4574
9.2	4720
10.2	5033
11.2	5316
12.2	5493
13.2	5544
14.3	5534
15.3	5545
16.3	5621
17.2	5729

Tab. 3.4b: Final 1D p-wave velocity model derived from real data (horizontal non-weighted average over all data) valid at SED station on line 09SN_12PLONS-P1 (left) resp. 0 and 40 on line -P2 (right).

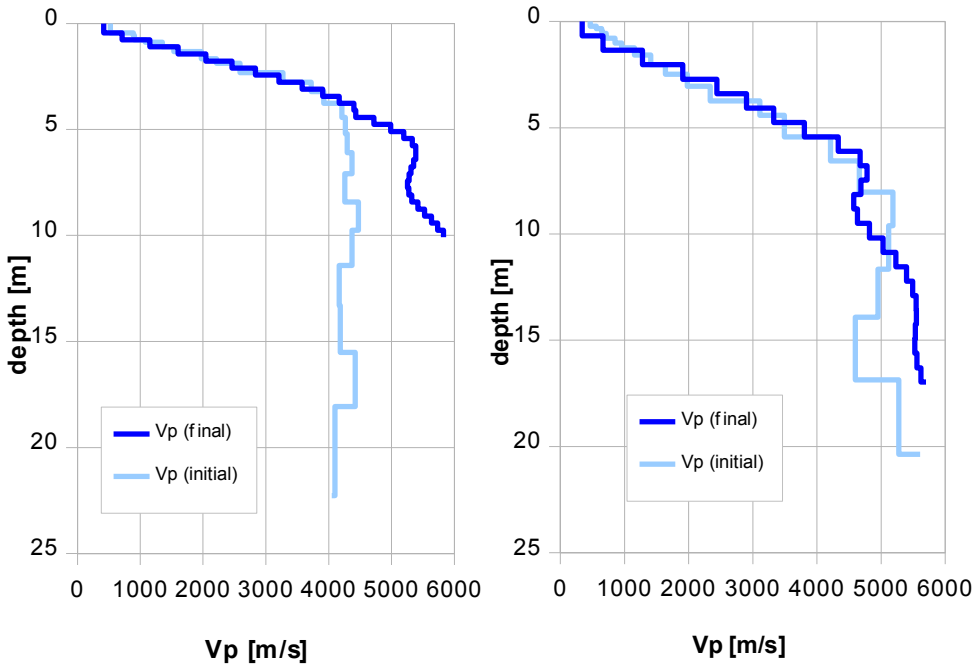

Fig. 3.4i: Final 1D p-wave velocity model derived from real data (horizontal non-weighted average over all data) valid at SED station on line 09SN_12PLONS-P1 (left) resp. 0 and 40 on line -P2 (right).

3.4.4 Representation of the hybrid seismic section

The hybrid seismic section is the reflection seismic section with the superimposed p-wave velocity field. It portrays the geological structures and the p-wave velocity field, the latter being indicative for the rock / soil rigidity. The uninterpreted hybrid seismic section is portrayed in Fig. 3.4j and 3.4k below.

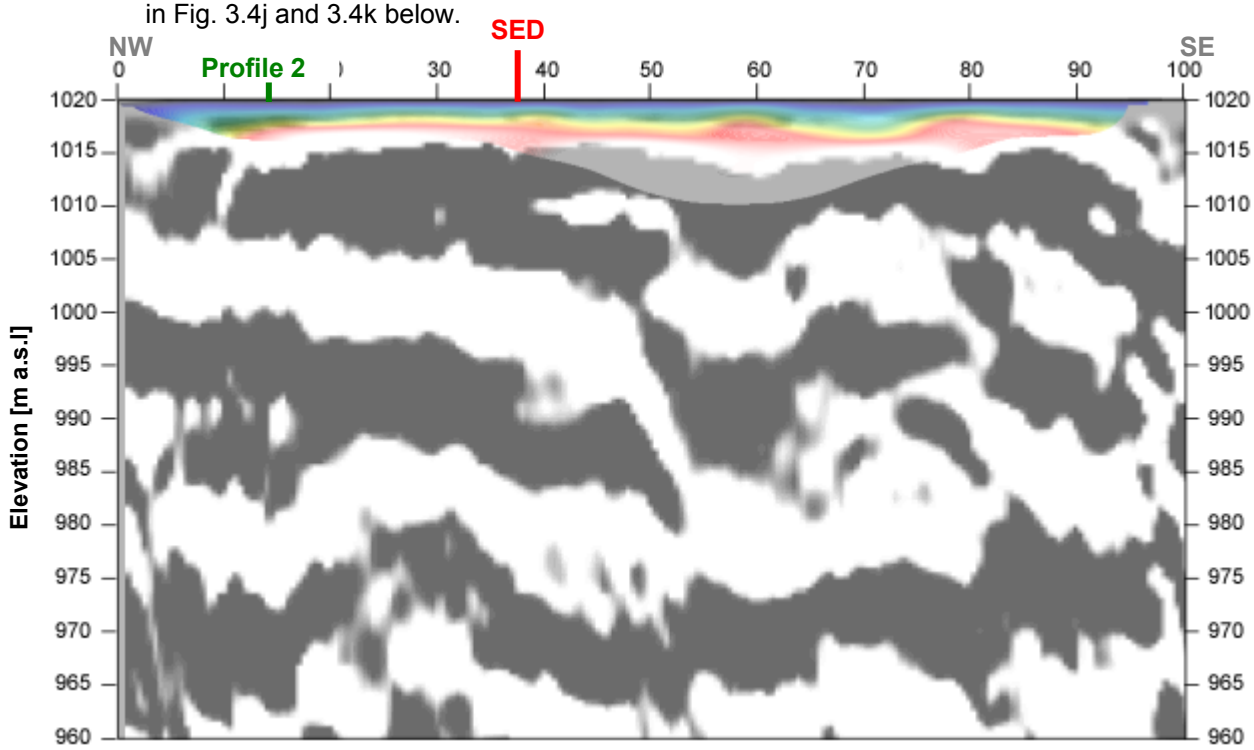

Fig. 3.4j Uninterpreted hybrid seismic section 09SN_12PLONS-P1: superimposed onto the seismic reflection section is the color encoded p-velocity field derived by refraction tomography (no vertical exaggeration).

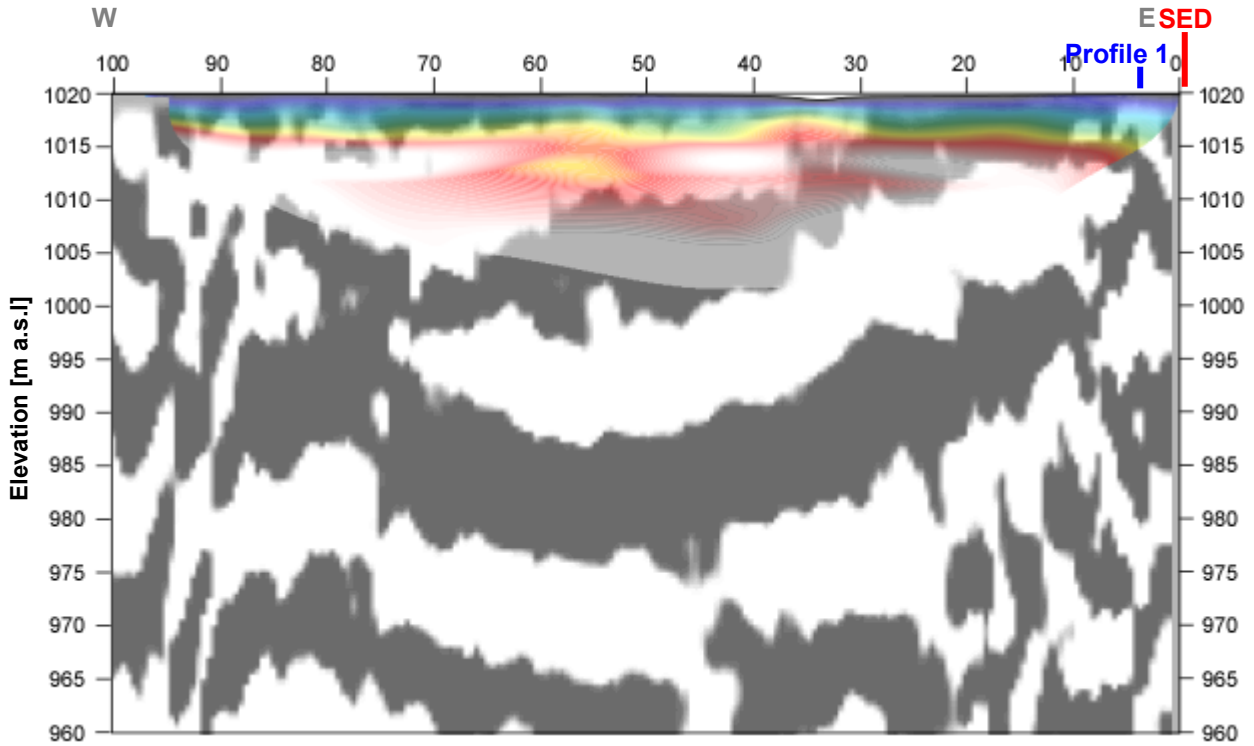

Fig. 3.4k Uninterpreted hybrid seismic section 09SN_12PLONS-P2: superimposed onto the seismic reflection section is the color encoded p-velocity field derived by refraction tomography (no vertical exaggeration).

4 DISCUSSION OF THE RESULTS

4.1 Summary and Validation of the Results

Compressional and shear wave velocity data from refraction seismic surveys both p-wave and s-wave and also the MASW survey data of profiles 09SN_12PLONS-1 and 09SN_12PLONS-2 are shown in Tab. 4.1 for the uppermost 30 m. The calculated shear wave velocity $v_{s(calc)}$ in Tab. 4.1 is derived by using a theoretical v_p/v_s-ratio of $\sqrt{3}$.

Depth	Vp1	Vp2	Vs1	Vs2	Vs1	Vs2	Vs1	Vs2
	meas	meas	meas	calc	meas	calc	MASW	MASW
0	417	339		241	475	196	1836	432
1	710		443	410		196	1861	819
2	2046	1280	587	1181	640	739	1851	634
3	3209	1909		1853		1102		
4	4167	2901	706	2406	854	1675	1788	734
5	4722	3325	1060	2726	1615	1920		
6	5329	4331		3076		2500	1692	747
7	5355	4675	1061	3092	1530	2699		
8	5256	4687		3034		2706		
9	5420	4574	951	3129	1113	2641	1636	713
10	5736	4630		3312		2673		
11		5033	929		1063	2906		
12		5228	947		1133	3019	1710	1067
13		5493				3171		
14		5546	975		1187	3202		
15		5534				3195		
16		5526	1020		1244	3191		1358
17		5621				3245	1921	
18			1153		1401			
19					2422			
20			1733					
21			2677		4281			1416
22							2070	
23			3418		5645			
24								
25			3169		5611			
26					5568			
27			3070					2363
28			3762					
29							2194	
30								

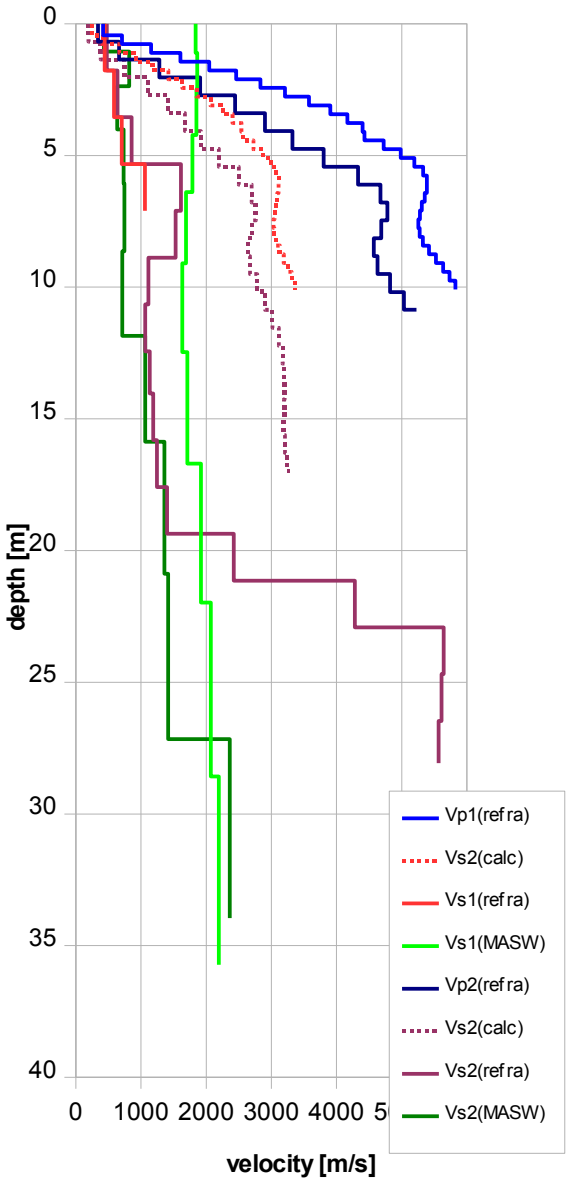

Tab. 4.1: Shear and compressional wave velocity model determined at the SED station PLONS.

Fig. 4.1: Graphic display of shear (red continuous lines) and compressional (blue lines) wave velocities determined at the SED station. Red dotted lines reflect from p-wave data calculated maximum shear wave velocity values. In green colors values of MASW analyses at the SED station.

4.2 Validation of the methods and their results

Due to methodological differences, v_s velocities derived by MASW analysis and by the refraction tomography technique may differ considerably. This is because MASW analysis cannot image small rock/soil inhomogeneities as a dispersion image with an array length of i.e. 40-m only yields one single v_s-value at each depth. On the other hand, refraction diving wave tomography results produce v_s-sections with a high lateral resolution, but fail to provide information at greater depths.

4.3 Error Estimates

The error estimates given in Tab. 4.3 below are relevant only in the context of this survey.

Surveying method	Type of result	Error estimate
v_s – refraction tomography+	v_s – velocity field image	20%
MASW only "+" or only "-" values*	v_s – velocity field image	20%
MASW (mean of "+" & "-" values)*	v_s – velocity field image	15%
v_p – refraction tomography	v_p – velocity field image	10%
Reflection seismic surveying	Image of subsurface structures	n.a.

** MASW values derived from line M2 array inversions are not reliable.*

Tab. 4.3 Error estimates for the methods applied. Note that higher error estimates are to be taken into account with increasing depths.

The above error estimates are of a qualitative character only. On seismic profile 09SN_12PLONS-1, the shear wave values derived by shear wave refraction tomography and MASW analyses coincide well. Also do the imaged structures by p-wave and shear wave tomographic wave fields. These datasets were collected along the gravel road, directly along the solid rock in contrast to the profile 09SN_12PLONS-2 where both the source and the receivers are some meters away from solid rock.

It seems, that this contrast in distance between seismic layout and solid rock make large differences in the quality of the obtained results.

4.4 The Geophysical Interpretation

The most conclusive information about the subsurface structures is provided by the results of the hybrid seismic section (v_p-refraction tomography profiling and reflection seismic section) and confirmed by the evaluation results of the v_s-refraction tomography data.

As can be seen from the v_s and v_p refraction tomography sections in Fig. 3.2e/f & Fig. 3.4g/h, the topography of the bedrock is imaged in less than 3 meters overall the profile, except in the most Northeastern part.

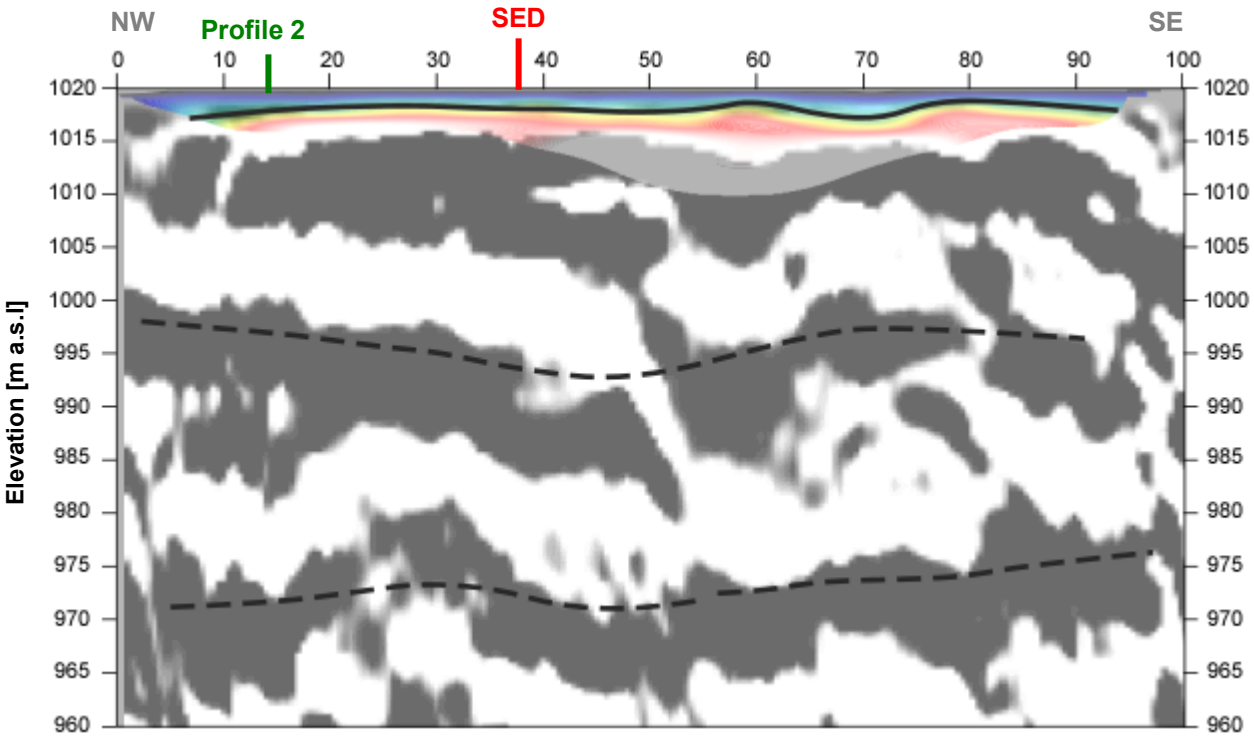

Fig. 4.2a Geophysical interpretation of the hybrid seismic section 09SN_12PLONS-P1. Black lines denote layer boundaries, continuous line the bedrock surface.

The geological interpretation of the seismic events of line 09SN_12PLONS-2 is shown in Fig. 4.2a. Similarly to the bedrock's topography in line 09SN_12PLONS-1, the topography of the bedrock surface is imaged in detail all over the profile, generally a bit deeper than on line 1.

The bedrocks layering shows a soft depression with the sole around profile meter 60.

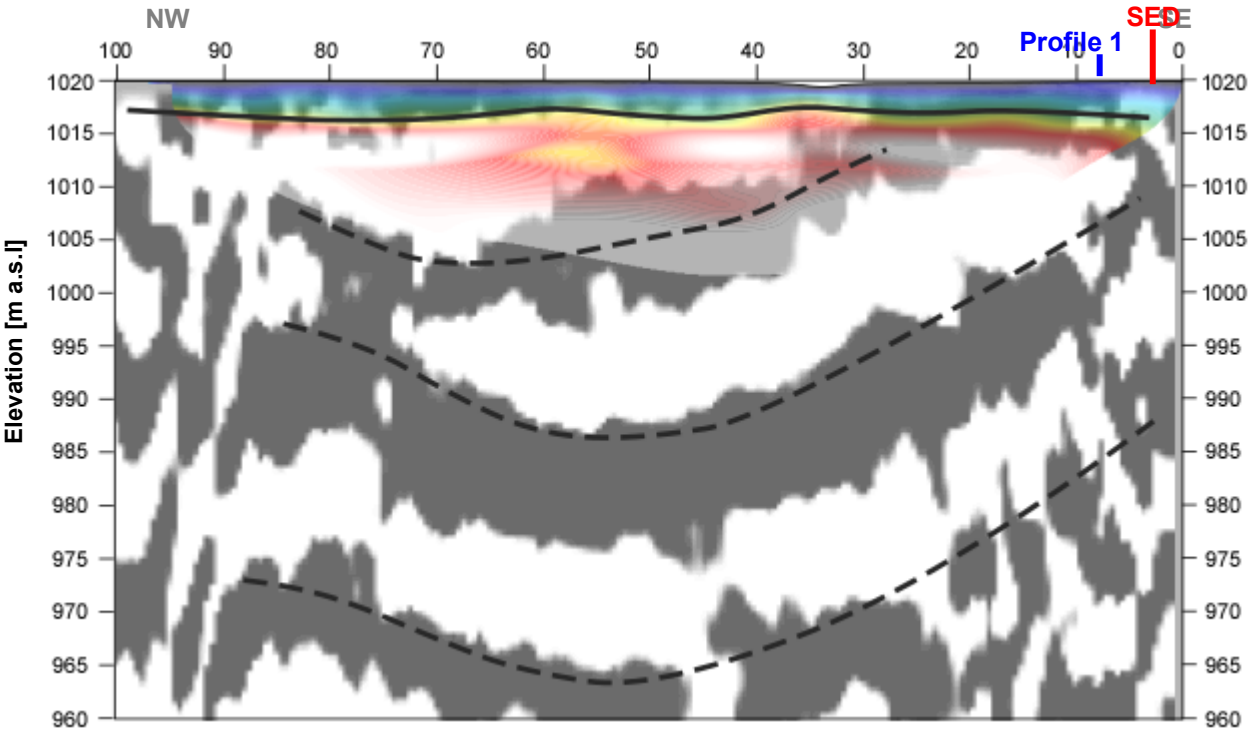

Fig. 4.2b Geophysical interpretation of the hybrid seismic section 09SN_12PLONS-P2. Black lines denote layer boundaries, the continuous one marks the bedrock surface.

5 SUMMARY AND CONCLUSIONS

- In May 2009 a combined seismic s- and p-wave survey was carried out at the SED earthquake monitoring station PLONS near Mels SG in the Swiss Eastern Prealps.
- The shear wave data have been evaluated by conventional diving wave refraction tomography techniques in order to derive the s-wave velocity field along the seismic line. Due to the inherent constraints of the refraction tomography method, the depth of reliable investigation is limited to less than 10 m under the prevailing geological conditions.
- The p-wave data have been processed
  - firstly to derive a 2D s-wave velocity field by using the MASW (**M**ultichannel **A**nalysis of **S**urface **W**aves) technique;
  - and secondly, according to the hybrid seismic data processing scheme for representing the subsurface structures in a combined reflection seismic section with the superimposed p-wave velocity field.
- The reliable shear wave velocity range determined by the MASW method (only line 09SN_12PLONS-M2) in the uppermost 30 meters spans from values of 1636 m/s to 2194 m/s.
- The scalar values derived by the MASW survey at the SED station (seismic line 09SN_12PLONS-M1, profile station 55; seismic line 09SN_12PLONS-M2, profile station 45) are the following:

line 1			line 2		
$v_{s,5}$	=	1836 m/s	$v_{s,5}$	=	641 m/s
$v_{s,10}$	=	1772 m/s	$v_{s,10}$	=	600 m/s
$v_{s,20}$	=	1709 m/s	$v_{s,20}$	=	734 m/s
$v_{s,30}$	=	1782 m/s	$v_{s,30}$	=	888 m/s
$v_{s,40}$	=	1830 m/s	$v_{s,40}$	=	n/a

- The reliable refraction shear wave velocity in solid rock derived is about 1600 m/s.
- The reliable p-wave velocity determined in solid rock is between 4500 m/s and 5300 m/s.
- The geophysical interpretation of the subsurface structures in this report are to be validated and incorporated into a comprehensive appraisal by a geologist familiar with the local geological setting.

Schwerzenbach, 7th July 2009

Walter Frei
dipl. Natw. ETH
managing director

Lorenz Keller
dipl. Natw. ETH
project manager